Examining Virulence Plasmid Loss in *Yersinia pseudotuberculosis*

Thesis submitted to the University of Nottingham for the degree of Master of Research

Jake Dunlop, B.Sc. (Hons)

September 2020

Abstract

The genus *Yersinia* is composed of eleven species, three of which (*Y. pseudotuberculosis*, *Y. enterolitica*, and *Y. pestis*) are human pathogens. It is believed that *Y. pseudotuberculosis* is the predecessor of *Y. pestis*, which causes plague, and as a result there is a close genetic link between the two species. Each of the pathogenic species possess an approx. 70 kb plasmid known as pYV, (pCD1 in *Y. pestis* and pYVe in *Y. enterocolitica*) which is essential for virulence. The plasmid codes for a Type III Secretion system (T3SS) composed of structural proteins which form an injectisome (analogous to a hypodermic needle) and effectors which when combined disarm host immune cells through disruption of processes such as actin polymerisation as well as inducing cellular apoptosis. Expression of these proteins, usually referred to as Yops, are known to be regulated by both the environment (through temperature and calcium concentration) and the bacterial cell-to-cell signalling system known as Quorum Sensing (QS).

The QS system plays an important role in the maintenance of the pYV plasmid within the population. Previous work has shown that transcriptional regulators and signal synthase mutants in the QS system are unable to secrete Yops, and virulence plasmid levels in a population fall rapidly in these mutants when compared to the parent. It is hypothesised that QS plays a key role in the maintenance of the pYV plasmid.

This study aims to investigate the link between QS and plasmid maintenance through the targeting of the *copA*/*copB* promoters. *copA* and *copB* both control the plasmid replication initiation protein RepA through repression of the *repA* gene. They play a key role in plasmid replication and therefore plasmid maintenance. *lux*-based reporter fusion technology was used, which contains a *luxCDABE* cassette, and *copA*/*copB* promoters. When gene expression occurs, light is emitted from the cell, which can be measured to indicate the level of this expression. The promoters of c*opA* and *copB* will be used as a marker for plasmid maintenance by examining expression in the parent and QS mutant backgrounds. These fusions were successfully created, however further data was not possible to obtain given the situation regarding the 2019-Novel-Coronavirus pandemic.

Acknowledgements

Firstly, I would like to thank my supervisors Steve Atkinson and Paul Williams for both giving me the opportunity to undertake this project, and for their continuous support and guidance throughout. Not only did they support me throughout my time in the laboratory, they have gone above and beyond to deal with the extreme difficulties caused by the 2019-Novel-Coronavirus pandemic that no doubt has changed not only the way in which my project finished, but the university and world beyond.

I would also like to acknowledge and thank Vanina Garcia and Clair Brooks for their exceptional technical assistance they provided throughout. I would also like to thank Vanina in particular for her help in both settling me into the laboratory, and providing advice in not only my project, but my future career/academic choices. Unfortunately, she had to part ways before the project came to its end and I wish her the best of luck in the future.

Outside of the laboratory, I must thank my family and friends for their continuous support throughout this difficult year. To my Mum, Dad, Brother and Girlfriend: thank you for keeping me going throughout with both helping me relax and ensuring I remained focussed while having to work from home in a different environment to what I may be used to when writing work such as this.

Abbreviations

Abbreviation	Description
AHL	*N*-acyl-homoserine lactone
Amp	Ampicillin
bp	Base pair
BHI	Brain heart infusion
Ca^{2+}	Calcium
^{o}C	Degrees Celsius
Cm	Chloramphenicol
DMSO	Dimethylsulfoxide
DNA	Deoxyribonucleic acid
dNTP	Deoxyribonucleotide triphosphate
FESLF	Far East Scarlet-Like Fever
g	Gram(s)
gDNA	Genomic DNA
Gm	Gentamicin
kb	Kilobase
Km	Kanamycin
l	Litre
LB	Lysogeny broth
min	Minute
mg	Milligram
ml	Millilitre
mM	Millimolar concentration
µM	Micromolar concentration
nM	Nanomolar concentration
µl	Microlitre
µg	Microgram
Nal	Nalidixic acid
ng	Nanogram
OD	Optical density
ori	Origin of Replication
par	Partition system
PCR	Polymerase chain reaction
pH	Potenz (power) of hydrogen
pYV	*Yersinia* virulence plasmid
QS	Quorum sensing
^{R}	Resistance
RNA	Ribonucleic acid
rpm	Revolutions per minute
s	Second(s)
SOB	Super Optimal Broth
Spp.	Species
TA	Toxin-antitoxin
TAE	Tris-acetate-EDTA buffer
TB	Terrific Broth

T3SS	Type-III-secretion system
V	Volts
WHO	World Health Organisation
w/v	Weight to volume
x	Times
x g	Times gravitational force
x-gal	5-bromo-4-chloro-3-indolyl-β-D-galactopyranoside
Yad	*Yersinia* adhesin

Table of Contents

1 Introduction 1

1.1 *Yersinia* background 1

1.1.1 The History, Epidemiology, and Current State of *Yersinia* 1

1.1.2 The *Yersinia* Genus 2

1.2 Virulence in *Yersinia* 3

1.2.1 Adhesins 3

1.2.2 Virulence Plasmid 4

1.2.3 Type III Secretion System 5

1.2.4 *Y. pestis* Additional Virulence Plasmids 7

1.3 Plasmid maintenance 8

1.3.1 General Plasmid Maintenance 8

1.3.2 Plasmid Maintenance in *Yersinia* 9

1.4 Quorum Sensing in *Yersinia* 10

1.5 Previous Work and Aims of This Study 12

2 Materials and Methods 13

2.1 Growth Media and Growth Conditions 13

2.2 Bacterial Strains and Plasmids 13

2.2.1 Bacterial Strains 13

2.2.2 Plasmids used 14

2.3 General Genetic Modification 15

2.3.1 Molecular Cloning 15

2.3.1.1 Plasmid Handling 15

2.3.1.2 Restriction Digests 15

2.3.1.3 Gel Electrophoresis and DNA Extraction 15

2.3.1.4 Ligation of Vector and Fragment 16

2.3.1.5 Transformation of DNA into Competent Cells 16

2.3.1.6 Heat-Shock Transformation 16

2.3.2 Polymerase Chain Reaction 16

2.4 Detection of Luminescent colonies 17

2.5 Conjugation 17

2.6 Growth Curve 18

3 Results 19

3.1 Amplification of *copA*/*copB* 19

3.2 Cloning of *copA*/*copB* into pGEM-T Easy 21

3.3 Subcloning of the *luxCDABE* cassette 22
3.4 Subcloning of *copA*::*luxCDABE*/*copB*::*luxCDABE* into pDM4.2 24
3.5 Subcloning of copA::luxCDABE/copB::luxCDABE into pHG327 25
4 Discussion 27
References 32

List of Tables

Table 2.1: Bacterial Strains used 13
Table 2.2: Plasmids used within the study. 14
Table 2.3: Primers used in this study 17

List of Figures

Figure 1.1: The global distribution of natural plague foci 2
Figure 1.2: A map of the *Y. enterolitica* serotype O:8 virulence plasmid pYVe8081 4
Figure 1.3: A diagram depicting the structural components of the *Yersinia* Ysc injectisome 5
Figure 1.4: The three stages of generalised plasmid partitioning 8
Figure 1.5: The repA plasmid maintenance system 10
Figure 1.6: A diagram encompassing the steps of the Gram-negative QS system 11
Figure 3.1: A gel of a gDNA extraction from *Y. pseudotuberculosis* YPIII Parent pYV^{+} (A) The PCR products of the amplified *copA* and c*opB* promoter regions (B) 20
Figure 3.2: The YPIII pB1 plasmid Rep Operon from *Y. pseudotuberculosis* 20
Figure 3.3: A gel before ligation of both inserts and vector (A) PCR confirmation of the creation of pJd1::c*opA* and pJd1::*copB* (B) 21
Figure 3.4: A plasmid map of pJd1::c*opA* (A) A plasmid map of pJd1::c*opB* (B) 22
Figure 3.5: A gel of the cleaned/extracted insert vectors before using them further (A) PCR products from the screening of pJd1:c*opA*::*luxCDABE* and pJd1:c*opB*::*luxCDABE* (B) 23
Figure 3.6: A plasmid map of pJd1:c*opA*::*luxCDABE* (A) A plasmid map of pJd1:*copB*::*luxCDABE* (B) 23
Figure 3.7: PCR confirmation of the presence of pJd2:c*opA*::*luxCDABE* positive cells (A) PCR confirmation of the presence of pJd2:*copB*::*luxCDABE* positive cells (B) 24
Figure 3.8: A plasmid map of pJd2:c*opA*::*luxCDABE* (A) A plasmid map of pJd2:*copB*::*luxCDABE* (B) 25
Figure 3.9: PCR screening for pJd3:*copA*::*luxCDABE* and pJd3:*copB*::*luxCDABE* 26
Figure 3.10: A plasmid map of the vector pHG327 26

1 Introduction

1.1 *Yersinia* background

1.1.1 The History, Epidemiology, and Current State of *Yersinia*

The genus *Yersinia* which belongs to the *Enterobacteriaceae* family, is composed of between eleven and twenty-seven different species, three of which are medically important (1; 2) Of these, the most historically significant is *Y. pestis* – the causative agent of plague. This organism has been responsible for an estimated 200 million deaths after spreading throughout the world numerous times, including three pandemics, one of which was the most fatal pandemic recorded to date – The Black Death (3).

Y. pseudotuberculosis is an enteric bacterium, attributed as the cause of Far East Scarlet-Like Fever (FESLF) – also known as Izumi fever in Japan. FESLF typically arises sporadically in the northern hemisphere (Europe, North America, Russia, and Japan). Whilst the number of cases worldwide are relatively low, it is a seasonal disease, peaking during winter (4). The organism is a zoonotic pathogen that is typically acquired following ingestion of contaminated food or water, however as the symptoms manifest as gastroenteritis, accurate epidemiological figures are difficult to gauge. Whilst *Y. pseudotuberculosis* is the cause of FESLF, it more commonly presents itself as Yersiniosis, a zoonotic sporadic gastrointestinal infection. However, the main causative organism of Yersiniosis is *Y. enterocolitica* (5). This may be a result of several factors – the first of these being the reservoirs both organisms reside in. *Y. enterocolitica* has a wide range of these including pigs, cattle, dogs, cats, and rodents. Whereas *Y. pseudotuberculosis*' range includes farm animals, rodents, and birds. The possibility of spreading via domestic pets increases the odds of this happening when handling them regularly versus wild animals that may not necessarily be in regular contact with humans. Another potential reason for *Y. enterocolitica* more commonly causing infection than *Y. pseudotuberculosis* is the former causes infection consistently whereas the latter is more seasonal and therefore most cases are seen in winter (6). *Y. enterocolitica* is spread via the faecal-oral route usually from animals – contaminated water, milk and food are the main source of infection and as such outbreaks occasionally occur from common exposure rather than person-to-person transmission (7).

Y. pestis is a zoonotic bacterium and as such is transmitted between animals (and humans) via fleas. Plague foci can currently be found in 33 countries (figure 1.1), with 10 countries reporting human cases between 2014-19. Hundreds of human cases of the plague do still occur along with a number of deaths, primarily in the Democratic Republic of Congo, Peru, and Madagascar (9). Whilst plague can be treated with antibiotics, it has a high case-fatality ratio of 30-100% when left untreated (dependent upon the location where the infection takes hold [10; 11]). There are three manifestations of plague – Pneumonic, Bubonic and Septicaemic plague – each with different clinical features. Each is the result of the organism infecting a different location in the body. Pneumonic plague is caused when *Y. pestis* infects the lungs, causing pneumonia; septicaemic plague is caused when the organism multiplies in the blood, causing septicaemia; bubonic plague is caused by the infection of lymph nodes,

leading to acute painful lymphadenitis (bubo) (13). As such, WHO class the organism as a re-emerging dangerous pathogen. This classification, and recent events in Madagascar (August to November 2017, 2348 cases of plague were confirmed, including 202 deaths), suggest that *Yersinia pestis* still requires significant attention (9; 12).

Figure 1.1: The global distribution of natural plague foci as of March 2016 where red indicates the presence of natural plague foci based on recent information and historical data. Source: (8)

1.1.2 The *Yersinia* Genus

Historically, *Y. pseudotuberculosis* has been attributed as the predecessor of *Y. pestis*, with the latter being a recently evolved near-identical subclone of the former. This event was thought to have occurred anywhere between 1,500 and 20,000 years ago (14). Both *Y. pseudotuberculosis* and *Y. pestis* belong to a single clade in the *Yersinia* phylogenetic tree (15), whereas *Y. enterocolitica* is on a different clade entirely. Since the divergence from *Y. pseudotuberculosis*, analysis has shown that *Y. pestis* has 32 newly acquired chromosomal genes and 2 newly acquired *Y. pestis*-specific plasmids. However, more significantly it appears 317 genes became pseudogenes or were deleted from *Y. pestis* – meaning up to 13% of *Y. pseudotuberculosis* genes are no longer functioning in *Y. pestis*. As a result of both reductive evolution via massive gene loss and extensive genome rearrangements, pre-existing gene expression pathways have been lost or modified. This may be more important than the newly acquired genes in the virulence of *Y. pestis* (16).

1.2 Virulence in *Yersinia*

1.2.1 Adhesins

Bacteria require adhesion for colonisation of host cells and tissues, contributing to bacterial pathogenesis. Bacterial adhesion allows bacteria to attach/adhere to other cells and surfaces (17). Adhesins are split into different categories dependent upon their structure, assembly pathways, and surface export mechanisms; in the case of the human pathogenic *Yersinia* adhesins, there are four categories – the most important adhesins being *Yersinia* adhesin A (YadA), and invasin (InvA). Both YadA and InvA fall into the autotransporter (AT) adhesins (18).

YadA is a non-fimbrial adhesin encoded on the pYV plasmid (with the exception of *Yersinia pestis*, in which it is a pseudogene and as a result is inactive) and is responsible for *Yersinia* contact with a variety of host cells such as macrophages and epithelial cells. YadA is expressed in abundance at 37^{o}C and above, coating the outer surface of the cell. It is apparent that this adhesin has multiple functions, which may include acting as a docking system for the organism when invading a host cell. This allows the T3SS injectisome to attach to the target cell and deliver effector Yops. It is an essential adhesin to *Y. enterocolitica* pathogenicity but not as essential to *Y. pseudotuberculosis* due to its role being interchangeable with invasin (18; 19; 20).

InvA is a chromosomally encoded adhesin that mediates both attachment and entry into host cells. It is also present in *Y. pseudotuberculosis* and *Y. enterocolitica,* but in *Y. pestis* it is an inactive pseudogene. Regulation of invasin occurs through temperature and, in the case of *Y. enterocolitica,* also pH – the peak expression is typically at pH 8 and 25^{o}C or at pH 5.5 and 37^{o}C (21). InvA binds to target receptors, known as β1-integrins on the host cell surface. Upon the binding of InvA, the integrins form clusters and as a result, the host cell cytoskeleton is rearranged, ultimately promoting phagocytosis – leading to the internalisation of the bacterial cell into the host epithelial cells (22; 23).

Another example of adhesin is the attachment-invasion locus (ail). Ail is a small β-barrel protein expressed in all three pathogenic *Yersinia spp.* but at varying temperatures – 37^{o}C in both *Y. pseudotuberculosis* and *Y. enterocolitica*, but also at 26^{o}C to a lesser extent in *Y. pestis*. It is an important factor that influences cell adhesion, promotion of Yop delivery to host cells, cell invasion and serum resistance (18; 21; 24). There are many other adhesins that are either minor or more specific to a particular spp. These include the pH 6 antigen (psa), Plasminogen activator (Pla) and YadB/YadC (21; 25).

1.2.2 Virulence Plasmid

The 3 human pathogenic strains of *Yersinia spp*. possess an approx. 70 kb virulence plasmid (pYV in *Y. pseudotuberculosis*, pYVe in *Y. enterocolitica*, and pCD1 in *Y. pestis*) which has been described as an anti-host genome. pYV (figure 1.2), also known as the Yop (*Yersinia* outer protein) regulon encodes proteins that are required for the survival and replication of *Yersinia* to occur within the host's lymphoid tissues during infection. The plasmid encodes for the Yop virulon which consists of Yop proteins and a type III secretion system (T3SS), also known as Ysc (27; 28). It is well documented that the virulence plasmid is absolutely necessary for virulence in *Yersinia*. Studies have shown that when pYV is absent *Yersinia* spp. exhibit a severe reduction or attenuation of virulence (29; 30; 31).

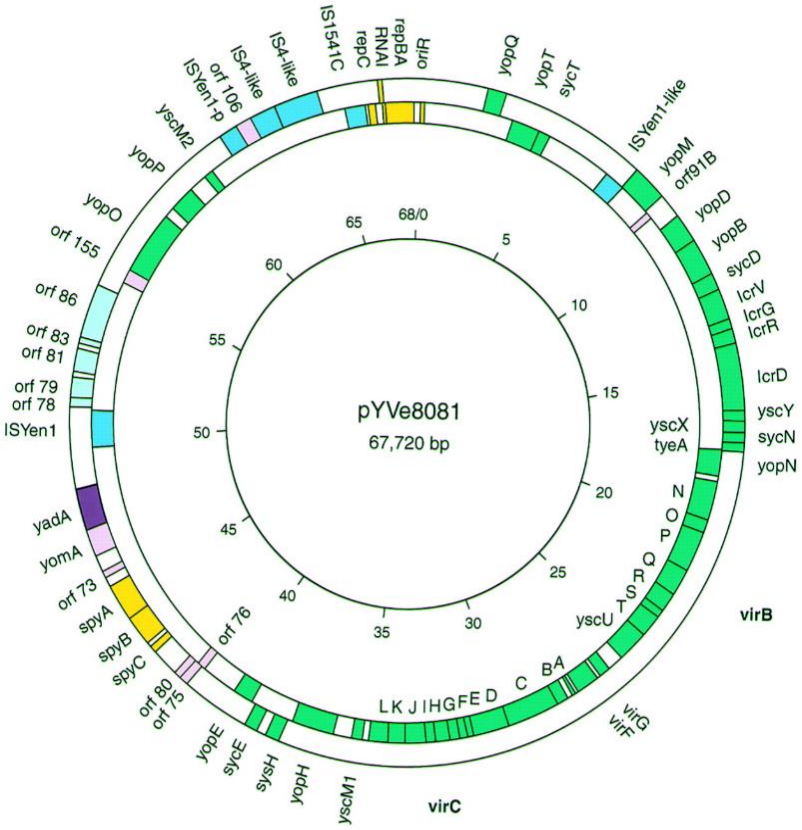

Figure 1.2: A map of the *Y. enterolitica* serotype O:8 virulence plasmid pYVe8081, indicating replication and partition regions, significant genes and IS elements. The inner circle indicates the scale of the plasmid in kb. The outer ring genes are transcribed anti-clockwise, with the inner ones being clockwise. Green indicates genes that make up the LCR (low calcium response) stimulon. Purple indicates *yadA* and genes linking to replication and partition functions are highlighted by yellow. Pink genes are those that have been previously identified but the function is unknown and potential new genes are indicated by light blue. Dark blue indicates IS elements. This plasmid is similar to pYV seen in *Y. pseudotuberculosis*, with a few minor differences including spyA, spyB, and spyC, rather than copA and copB seen within pYV. Along with this, pYVe also contains an additional Yop effector – YopT. Source: (26).

The Yop virulon allows the bacteria to disarm the host's immune cells by disrupting their communication, or via inducing cellular apoptosis by injecting the effector proteins into the cell. There are 2 categories of Yop proteins – intracellular effectors, and those that form the translocation apparatus. The Yops involved in forming the translocation apparatus are deployed at the bacterial surface to deliver their effectors into eukaryotic cells via their plasma membrane. When the bacteria come into contact with eukaryotic cells, the Yops are secreted and controlled by virulon proteins, which are thought to form a plug complex and close the bacterial secretion channel (27; 28; 32).

1.2.3 Type III Secretion System

The Ysc injectisome (figure 1.3) spans the two bacterial membranes and the peptidoglycan layer, whilst also protruding from the bacteria. The injectisome can be split into three sections: the basal body, the needle, and the pore complex (33). The basal body is formed through a series of ring structures, starting with the scaffold proteins. A ring is formed of YscC in the bacterial outer membrane. This is followed by another larger ring formed on the inner membrane consisting of YscD and YscJ (MS ring). The basal body is anchored into the peptidoglycan layer by the rings connecting to one another – hence the scaffold name. (34;

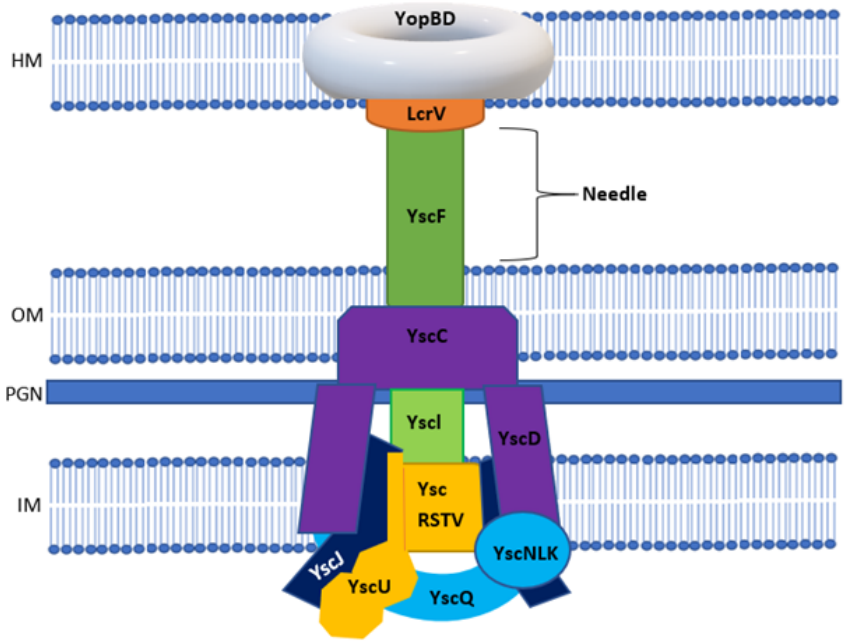

Figure 1.3: A diagram depicting the structural components of the *Yersinia* Ysc injectisome. The basal body where the injectisome sits is made up of the inner membrane (IM), peptidoglycan layer (PGN) and the outer membrane (OM). The needle tip complex (LcrV) and translocation pore (YopB/YopD) can be seen piercing the host membrane (HM). Purple/Dark blue indicates scaffold proteins: YscC, YscD, YscJ; Blue indicates cytoplasmic components: YscQ (C-ring) and YscN, YscL, YscK (ATPase complex); Green indicates: YscI (rod) and YscF (needle); light orange indicates export apparatus proteins: YscR, YscS, YscT, YscU and YscV; Dark orange/white indicates the pore complex: LcrV (needle tip complex) and YopB/YopD (translocation pore). Adapted from (28; 29).

35). YscN, YscL and YscK form an ATPase complex whilst the C ring forms, comprised of YscQ. Both these components associate with the scaffold proteins, at which point the basal body is almost complete (36). Meanwhile in a separate pathway, YscRSTUV assembles within the inner membrane separately from the scaffold proteins. This is the beginning of the export apparatus. The two assembly pathways then crossover as YscJ, within the MS ring, recruits the export apparatus. Once the export apparatus and ATPase complex have joined the scaffold, the basal body is complete and can begin to export secretion substrates (33; 37).

The rest of the construction of the Ysc injectisome can be split into three stages: early, middle, and late. The early stage begins following the completion of the basal body, where early substrates are translocated. These substrates include YscP, YscI, YscF, YscX, YscO, and YopR (38). YscI forms a substrate passage across from the inner membrane to the outer membrane. Once the passage is formed, YscF is secreted, which forms the injectisome needle through polymerization. YscP is known to regulate the length of the needle, whilst YopR is important for the early stages of needle assembly (the precise reasons for this are unclear) (38; 39). The individual roles of YscXYO are all unknown, though they are thought to be required for the export of these early substrates. YscP also has another role in which it interacts with YscU in the export apparatus upon completion of the needle. This causes YscU to undergo autocleavage, triggering a substrate specificity switch – leading to the middle stage (33; 40; 41).

Translocators ('middle' Yops), including YopB, YopD, and LcrV are secreted throughout the middle stage prior to cell contact. LcrV is secreted and polymerizes at the end of the needle to form a needle tip complex (figure 1.3) (33; 42). The translocation pore proteins (YopB and YopD) use the needle tip complex as a platform to insert themselves into the host cell membrane and combine to form a multimeric complex, at which point the transition to late stage secretion can be made (41; 42; 43).

The T3SS is activated at a temperature of 37^{o}C, alongside the presence of millimolar concentrations of calcium (Ca^{2+}) – conditions which represent a mammalian hosts' intracellular environment. It is believed that the formation of the LcrG-LcrV complex is important for Ca^{2+} regulated secretion of YopM (44; 45).

To prevent the degradation of the T3SS proteins, and prevent premature oligomerisation, specific chaperones are required. Class I chaperones assist the effector Yops, class II chaperones assist the pore-forming translocators and class III chaperones associate with needle subunits (46; 47).

Following adhesion and attachment to a host cell, the T3SS transfers a variety of virulence factors into the eukaryotic target cell. These factors, which are present in all three pathogenic *Yersinia* spp. are known as *Yersinia* effector proteins. They are synthesised within the bacterial cytoplasm and are eventually translocated via the T3SS. Four of these proteins (YpkA, YopE, YopT, and YopH) function to disrupt the cytoskeleton of host cells. YpkA, YopE and YopT also carry out the targeting of an important group of cell signalling components that are involved in phagocytosis. YpkA (or YopO in *Y. enterocolitica*) inhibits phagocytosis following association with RhoA family proteins; it binds to and phosphorylates actin, which is then used by *Y.*

enterocolitica for the titration of host regulators that are responsible for actin polymerisation (48; 49). YopE is a mimic of the GTPase-activating proteins for eukaryotes and as a result has the ability to disrupt the actin cytoskeleton, which in turn inhibits phagocytosis (45; 48). YopT cleaves post-translationally modified Rho GTPases (supressing RhoA mediated signalling), preventing the phagocytic cup (important in bacterial internalisation) from forming (50). This protein also inhibits the assembly of focal adhesion complexes, which are essential for macrophage migration (51). YopH is a multi-functional protein that disrupts pathways linked to both innate and adaptive immunity. Following the binding of YadA/Invasin to β1-integrins, YopH prevents autophagy; it also prevents macrophages from carrying out phagocytosis by phosphorylating focal adhesion complex proteins – this disrupts any links to the actin cytoskeleton (25; 48; 49).

Another two effectors (YopJ and YopM) downregulate features of the immune system. YopJ (or YopP in *Y. enterocolitica*) is an acetyltransferase that catalyses the acylation of kinases, which inhibits their ability in the activation of the release of NF-Kβ (an inducer of pro-inflammatory cytokine production) (41; 52). It was also discovered that YopJ holds an important role through inhibition of caspase-1 within macrophages (53). Lastly, YopM is translocated directly inside macrophages and it has been suggested that it can self-deliver into certain human cells (54). Although not fully characterised, it is theorised that YopM may interact with and down-regulate a number of pro-inflammatory cytokines. It is also suggested that it counteracts the innate immune system through encouraging the depletion of natural killer cells in several environments throughout a host, along with binding to caspase-1, preventing pyroptosis (25; 49; 55; 56)

1.2.4 *Y. pestis* Additional Virulence Plasmids

Yersinia pestis possesses two additional virulence plasmids – pPCP (also known as pPst) and pMT (also known as pFra). pPCP encodes for the plasminogen activator Pla protease/adhesin, which converts plasminogen to plasmin. Plasmin causes degradation of extracellular matrices, allowing the rapid invasion of host cells (57). Along with encoding for the surface protein Pla, pPCP encodes for the pesticin activity protein (Pst) and pesticin immunity protein (pim). Pesticin is a protein toxic to closely related bacterial strains including *Y. pestis*, *Y. enterocolitica*, *Y. pseudotuberculosis* and some *Escherichia coli* strains. Pim gives the organism immunity against its own pesticin by decreasing the sensitivity of the organism to the protein, preventing suicide via pesticin (57; 58). Whilst similar to a toxin/antitoxin system, the aim is to destroy other organisms rather than for plasmid maintenance. pMT encodes for the production of a murine toxin (Ymt), which is important for the colonisation of fleas (59).

1.3 Plasmid maintenance

1.3.1 General Plasmid Maintenance

Maintaining a stable plasmid copy number across a dividing bacterial population is essential to prevent plasmid loss during partition of newly replicated plasmids to daughter cells during cell division. If the plasmid(s) is not successfully transferred to both daughter cells those without the plasmid have a lower metabolic load and as a result can outcompete those possessing the plasmid. This can lead to an organism losing a plasmid over time if the environmental conditions do not apply sufficient selective pressure. Conversely, high stress environments may force bacteria to retain their plasmids (60; 61).

One of the most common systems employed to ensure a stable plasmid population is maintained, is through the *par* system, consisting of a centromere-like DNA site and two different proteins: a centromere-binding protein and a partition NTPase. There are three types of partition system. The type I *par* loci encodes for a Walker motif-containing ATPase; type II encodes actin-like proteins, and type III encodes for tubulin-like proteins (62; 63; 64; 65). These mechanisms are present in a variety of low copy-number plasmids as these plasmids are typically too large to copy in great numbers.

The general mechanism for *par* systems can be split into three different steps (figure 1.4), the first of which requires multiple centromere-binding proteins to bind to the centromere. This goes onto form the partition complex, which is a higher order nucleoprotein complex. The second step is where the plasmids within the cell pair together. The final step involves the partition complex recruiting a partition NTPase, which directs plasmid separation to opposite poles of the bacterial cell from their pair (62). This leads to the need for close control of the location of the few plasmids they possess. High-copy number plasmids are another mechanism to avoid plasmid loss. These plasmids are copied in huge numbers, reducing the chances of a daughter cell being produced without a plasmid. In theory if plasmids are distributed randomly in a cell, the probability of losing this plasmid is linked directly to the

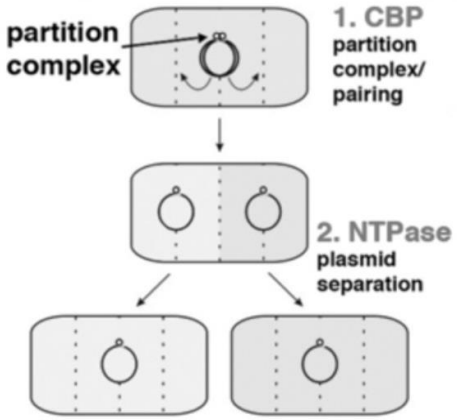

Figure 1.4: The three stages of generalised plasmid partitioning. The partition complexes are formed and the plasmids (represented by circles) pair up [1], before the NTPase molecules interact with the complexes and mediate plasmid separation [2] before cell division occurs. Source: (62)

number of copies. However, there are pitfalls with this as there is an increase in the metabolic load on the cell (66; 67).

Another approach taken is plasmid-free cell removal which involves the killing and/or growth inhibition of cells lacking plasmids. The first of these approaches is complementation of chromosomal mutation. An essential part of chromosomal DNA is encoded on the plasmid rather than the chromosome itself. As a result, cells lacking the plasmid cannot grow (68). Another way in which this approach can be taken is through environmental selection. Environmental changes/cues can impact a population in a variety of ways and this system uses environmental cues that would usually kill cells to its advantage. Those with the plasmid may have some in-built environmental response or resistance to deal with these changes, but those that are plasmid-free are unable to grow (68; 69). Lastly the post-segregational killing system, also known as the toxin-antitoxin (TA) system is used to kill plasmid-free cells. In this case the plasmid takes an active role to kill the daughter cells while preserving those that contain the plasmid. These systems encode for both a toxin and the corresponding antitoxin. The plasmids produce both the stable toxin and unstable antitoxin to counteract it. This leads to the cells that possess the plasmid surviving and those without the plasmid/antitoxin die. Five classes of TA systems have been discovered thus far, each with slightly differing mechanisms but the same outcome (70).

1.3.2 Plasmid Maintenance in *Yersinia*

Yersinia use a type I *par*, and in some cases also TA systems, to prevent plasmid loss from occurring. The type I *par* consists of the genes *parA*, *parB*, and *parS*. An operon is formed out of the genes *parA* and *parB* with the partition site *parS* directly downstream. The protein ParB and double-stranded DNA stimulate the ATPase ParA (71; 72; 73; 74).

TA systems have been observed in both *Y. enterocolitica* and *Y. pestis* (a combination of the HigBA, HicAB, MqsRA, Phd-Doc, and RelBE families of TA system that have been identified in the chromosome of the CO92 strain) but not *Y. pseudotuberculosis* (75; 76; 77). Whilst some information is known about TA systems within *Yersinia*, they remain largely uncharacterised. However, sequencing has shown that a ParDE family TA system is common within some *Yersinia* spp. plasmids, most notably pCD1 in *Y. pestis* and the chromosome of *Y. enterocolitica*. While it is believed these play a role in plasmid maintenance, the extent of this contribution and the biological role of the system required further investigation (78).

The replicase RepA has control over the copy number of the pYV plasmid to ensure there is a balance between enough plasmids to avoid plasmid loss but not too many so that the metabolic load is too heavy. The protein RepA consists of two domains, an N-terminal and a C-terminal (79; 80). RepA initiates replication at the *ori*, though how the protein acts down to a molecular level is unknown. As a result of its role, RepA is negatively regulated at both a transcriptional and post-transcriptional level through repression by CopA and CopB in the absence of host cells. The transcriptional repressor CopB interacts with the *repA* promoter, preventing *repA* from being activated. Meanwhile, the antisense RNA (asRNA) CopA prevents translation of signal peptides (which are required for RepA translation) as it binds to the 5' end of the longer of two *repA* transcripts (figure 1.5) (78; 81; 82; 83).

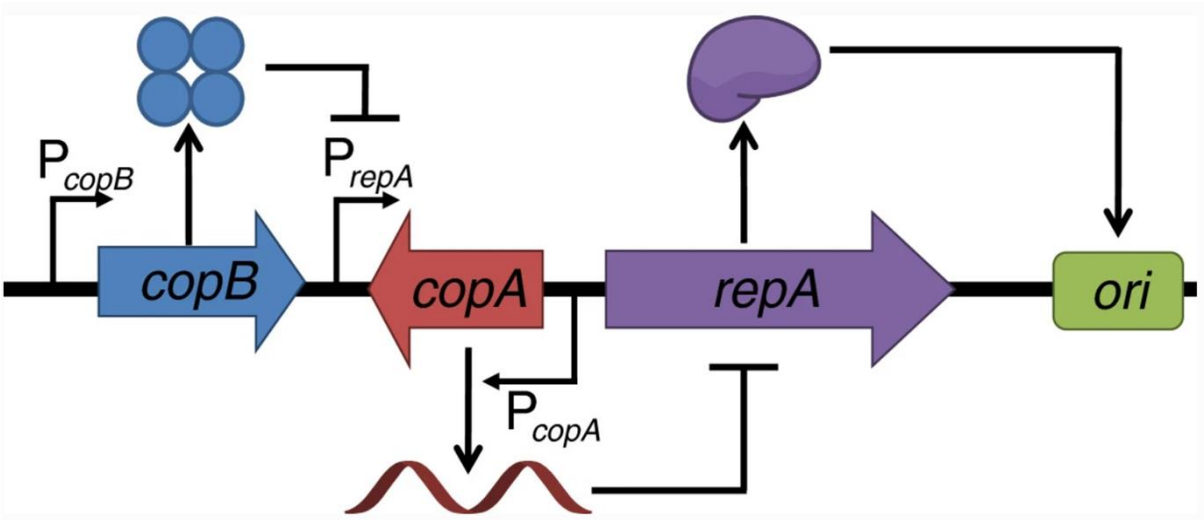

Figure 1.5: The RepA plasmid maintenance system. RepA binds to and activates the origin of replication (*ori*), however in the absence of host cells, CopB interacts with the *repA* promoter – preventing its activation. The non-coding RNA CopA is antisense to repA and acts post-transcriptionally - preventing the translation of signal peptides required for *repA* translation. Source: (84)

1.4 Quorum Sensing in *Yersinia*

Quorum sensing (QS) is a mode of cell-to-cell communication, used to promote collective behaviour within a population (seen in both Gram-positive and Gram-negative bacteria along with eukaryotic organisms) and is driven by the production and transduction of signal molecules in a population density dependent manner. The larger the density, the greater the overall synthesis of the signal molecules and once the signal reaches the required threshold concentration, the initiation of a signal transduction cascade is triggered. At this point a population-wide change in behaviour occurs in response to the messages spread. Some examples of these messages include information around population density, the environment, metabolism and motility (85; 86; 87; 88; 89; 90).

One of the first discovered examples of this is the marine bacterium *Vibrio fischeri*, in which the acyl homoserine lactone (AHL) synthase *luxI* encodes for the AHL synthase, whilst the *luxR* gene encodes for AHL binding and transcriptional activator LuxR. Observations have found that at higher cell density bioluminescence increases (83; 92; 93).

These AHL signal molecules diffuse or are actively transported out of the cell into the extracellular environment and as the population density of the bacteria increases, so does the concentration of signalling molecules. Once the threshold concentration is reached, the molecules re-enter the cell and bind with the LuxR homologue receptor proteins (87). The AHL/LuxR homologue then binds to the promoter region of the *lux* box, which induces the expression of genes downstream. In this case the genes *luxCDABE* are activated, resulting in bioluminescence (92; 93). This establishes a positive feedback loop that then promotes synchronised gene expression within the bacterial population (94; 95) (figure 1.6).

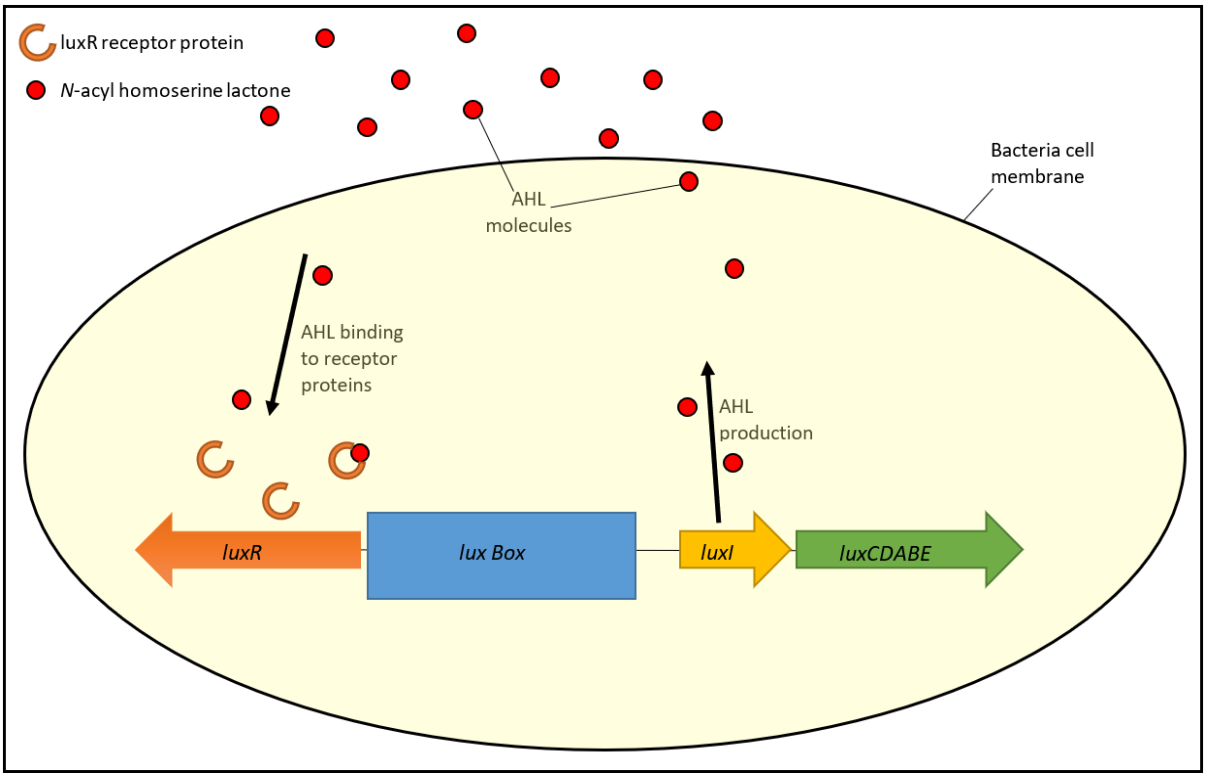

Figure 1.6: A diagram encompassing the steps of the gram-negative QS system within a bacterial cell when the threshold concentration of AHL signalling molecules is reached. Adapted from (91).

In *Yersinia*, a similar set of orthologs are in use. In *Y. pseudotuberculosis* there are two sets, known as *ypsI* and *ytbI* (AHL synthase genes), and *ypsR* and *ytbR* (transcriptional regulators). Similarly, *Y. pestis* has two pairs of orthologs, which are *yspI*/*yspR* and *ypeI*/*ypeR* (86; 96). Lastly, in *Y. enterocolitica* there is a single pairing of *yenI*/*yenR* (88). The system in *Yersinia* works in an analogous fashion to the *Vibrio fischeri* QS system. However, there is crossover between each of the pairings as the system is arranged in a hierarchical structure. For example, in *Y. pseudotuberculosis* the YpsR protein regulates the *ytbR*/*I* locus, indicating the orthologs overlap in terms of regulation (97).

The YpsR/YpsI and YtbR/YtbI QS systems in *Y. pseudotuberculosis* were found to fine tune motility through influencing the expression of *flhDC* and *fliA*, which are both key regulators of the motility cascade (97). This relationship is similar within *Y. enterocolitica*, but *Y. pestis* is non-motile and as a result the association between QS and the motility cascade regulators may be different when compared to both *Y. pseudotuberculosis* and *Y. enterocolitica* (88; 98; 99). The relationship between QS and biofilm formation has also previously been investigated, specifically on the nematode *Caenorhabditis elegans*. The investigation suggested a link between the two as AHLs were produced in nematode associated biofilms and AHL synthase/transcriptional regulator genes mutated within *Y. pseudotuberculosis* strains or those expressing AHL-degrading enzymes lead to attenuation of biofilm formation (86). QS also has an important role in the T3SS, through repression rather than the positive regulation seen in motility. Evidence for this was provided through the mutation of flagellar components (*flhDC*, *flhA* and *fliA*) and multiple QS genes (such as *ytbI*, *ypsR*, *ytbR* and the double mutants

ypsR/*ytbR* and *ytbI*/*ypsI*) (86). It has recently been suggested that *lcrF* (Also known as VirF in *Y. enterocolitica*) is negatively regulated by QS and that *ymoA* is positively regulated at both 22^{o}C and 37^{o}C (100). LcrF is a temperature-regulated activator of the pYV Yop regulon and is key to the assembly, and regulation of the T3SS (along with regulating *yadA* expression), in both *Y. pseudotuberculosis* and *Y. enterocolitica* (101; 102). YmoA is a histone-like protein that modulates the expression of *lcrF* and as a result is also key to virulence in *Yersinia* (103)

1.5 Previous Work and Aims of This Study

Whilst not fully established, the link between QS and virulence plasmid maintenance has been suggested. Data gathered on *Y. enterocolitica* suggested QS plays a role during infection through the regulation of pYVe partition via SpyA (present in *Y. enterocolitica* and homologous to ParA/CopA). Naturally, the data also evidenced a link between QS and plasmid loss, highlighted when comparing pYVe plasmid loss in both a parent and *yenI* mutant strain. The *yenI* mutant (the same as the parent strain but lacking the y*enI* gene) had a higher rate of plasmid loss when compared to the parent, indicating QS plays a role in plasmid maintenance, and as a result also plasmid loss. However, more work is required to understand the contribution of QS down to a molecular basis (88).

To begin filling this gap in our current knowledge, the aim of this study was to investigate the link between QS and plasmid maintenance through the targeting of *copA*/*copB* promoters. Both *copA* and *copB* negatively regulate the replicase gene *repA*, which controls the copy number of the pYV plasmid (figure 1.5). As a result, c*opA* and *copB* play a key role in controlling plasmid loss/maintenance (81; 82). If QS is related to the promotion of these genes, it can be confirmed that QS does play a role in plasmid maintenance/loss.

2 Materials and Methods

2.1 Growth Media and Growth Conditions

E. coli strains were grown at 37°C, shaking at 200 rpm in LB broth (104) unless otherwise stated. *Y. pseudotuberculosis* strains were grown at 30°C in YLB broth (105) shaking at 200 rpm. Appropriate antibiotics were added at the following concentrations: chloramphenicol (Cm) 10 µg / ml, gentamicin (Gm) 10 µg / ml, nalidixic acid (Nal) 22.5 µg / ml, and ampicillin (Amp) 100 µg / ml. When grown on plates 15 g / l agar was added to the media.

2.2 Bacterial Strains and Plasmids

2.2.1 Bacterial Strains

All bacterial strains used throughout this study are listed in Table 2.1.

Table 2.1: Bacterial Strains used

Bacterial Strain	Description	Source
	E. coli	
DH5α	*E. coli* K-12 cloning strain, (Amp^R)	(106)
S17-1 λ–*pir*	A host capable of transferring suicide plasmids requiring the Pir protein via conjugation	(107)
S17-1 λ–*pir* pDM4.2	S17-1 λ–*pir* containing the suicide vector pDM4.2 (Gm^R)	(107)
pHG327	An *E. coli* strain containing the vector pHG327	(108)
	Y. pseudotuberculosis	
YpIII Parent pYV^+	*Y. pseudotuberculosis* parent strain possessing the virulence plasmid pYV, Serotype O:3 (Nal^R)	(109)
YpIII Parent pYV^-	Parent *Y. pseudotuberculosis* strain cured of the virulence plasmid Serotype O:3 (Nal^R)	(110)
YpIII ΔII	*Y. pseudotuberculosis* strain lacking the QS synthases *ypsI* and *ytbI* (Cm^R, Km^R)	(97)
YpIII ΔRR	*Y. pseudotuberculosis* strain lacking the QS transcriptional regulators *ypsR* and *ytbR* (Cm^R, Km^R)	(97)
	Promoter Fusions	
DH5α pJd1::*copA*	DH5α harbouring the plasmid pJd1::*copA*	This Study

DH5α pJd1::*copB*	DH5α harbouring the plasmid pJd1::*copB*	This Study
DH5α pJd1::*copA*::*luxCDABE*	DH5α harbouring the plasmid pJd1::*copA*::*luxCDABE*	This Study
DH5α pJd1::*copB*::*luxCDABE*	DH5α harbouring the plasmid pJd1::*copB*::*luxCDABE*	This Study
S17-1 λ–*pir* pJd2::*copA*::*luxCDABE*	S17-1 λ–*pir* containing the plasmid pJd2::*copA*::*luxCDABE*	This Study
S17-1 λ–*pir* pJd2::*copB*::*luxCDABE*	S17-1 λ–*pir* containing the plasmid pJd2::*copB*::*luxCDABE*	This Study
YPIII Parent pYV$^+$ pJd2:*copA*::*luxCDABE*	YPIII Parent pYV$^+$ with integrated pJd2:*copA*::*luxCDABE* plasmid	This Study
YPIII Parent pYV$^+$ pJd2:*copB*::*luxCDABE*	YPIII Parent pYV$^+$ with integrated pJd2:*copB*::*luxCDABE* plasmid	This Study
YPIII ΔII pJd2:*copA*::*luxCDABE*	*Y. pseudotuberculosis* strain lacking the QS synthases ypsI and ytbI with the presence of the plasmid pJd2:*copA*::*luxCDABE*	This Study
YPIII ΔII pJd2:*copB*::*luxCDABE*	*Y. pseudotuberculosis* strain lacking the QS synthases ypsI and ytbI with the presence of the plasmid pJd2:*copB*::*luxCDABE*	This Study
YPIII ΔRR pJd2:*copA*::*luxCDABE*	*Y. pseudotuberculosis* strain lacking the QS synthases *ypsR* and *ytbR* whilst harbouring the plasmid pJd2:*copA*::*luxCDABE*	This Study
YPIII ΔRR pJd2:*copB*::*luxCDABE*	*Y. pseudotuberculosis* strain lacking the QS synthases *ypsR* and *ytbR* whilst harbouring the plasmid pJd2:*copB*::*luxCDABE*	This Study
S17-1 λ–pir pJd3:*copA*::*luxCDABE**	S17-1 λ–*pir* containing the plasmid pJd3:*copA*::*luxCDABE*	This Study
S17-1 λ–pir pJd3:*copB*::*luxCDABE**	S17-1 λ–*pir* containing the plasmid pJd3:*copB*::*luxCDABE*	This Study

*Designed only

2.2.2 Plasmids used

Every plasmid used in this study is listed in Table 2.2.

Table 2.2: Plasmids used within the study.

Plasmid	Description	Source
pGEM-T-easy	Cloning vector (Amp^R)	Promega©
pBlue*lux*	pBluescript II KS$^+$ Vector containing the luxCDABE operon (Amp^R)	(98)
pHG327	Low copy number vector (Amp^R)	(108)

pDM4.2	*Pir* protein reliant suicide vector	Joanne Purves (Unpublished)
pJd1::*copA*	Amplified CopA promoter integrated into the cloning vector pGEM-T-Easy (Amp^R)	This study
pJd1::*copB*	Amplified CopB promoter integrated into the cloning vector pGEM-T-Easy (Amp^R)	
pJd1:*copA*::*luxCDABE*	The cloning vector pGEM-T-Easy housing the amplified PcopA and the *luxCDABE* cassette (Amp^R)	This study
pJd1:*copB*::*luxCDABE*	The cloning vector pGEM-T-Easy housing the amplified PcopB and the *luxCDABE* cassette (Amp^R)	This Study
pJd2:*copA*::*luxCDABE*	The *Pir* protein dependent suicide plasmid pDM4.2 harbouring the amplified PcopA and the *luxCDABE* cassette (Gm^R)	This study
pJd2:*copB*::*luxCDABE*	The *Pir* protein dependent suicide plasmid pDM4.2 harbouring the amplified PcopB and the *luxCDABE* cassette (Gm^R)	This Study
pJd3:*copA*::*luxCDABE**	The vector pHG327 containing both amplified PcopA and the *luxCDABE* cassette (Amp^R)	This study
pJd3:*copB*::*luxCDABE**	The vector pHG327 containing both amplified PcopB and the *luxCDABE* cassette (Amp^R)	This Study

*Designed only

2.3 General Genetic Modification

2.3.1 Molecular Cloning

2.3.1.1 Plasmid Handling

The Sigma GenElute™ Plasmid Miniprep Kit was used for the extraction of plasmids throughout. Extracted plasmids were eluted in H_2O and stored at -20°C, unless stated otherwise. The manufacturer's instructions were followed throughout.

2.3.1.2 Restriction Digests

Restriction enzymes (Promega) were used in accordance to the supplier's instructions for the digestion of plasmids as described by Schagat *et al*. (111).

2.3.1.3 Gel Electrophoresis and DNA Extraction

When performing gel electrophoresis, agarose gels (1.2% (w/v) agarose, 1 x TAE buffer [50 x stock solution: 2.0 M Tris-acetate pH 8, 0.05 M ethylene-diamine-tetraacetic acid – EDTA]) were used. Each gel contained 0.1 µl/ml SYBR™ Safe gel stain. Wells were loaded with 6 µl – 25 µl DNA in 6x Promega loading dye and were run alongside DNA ladder (100 bp ladder or 1 kb ladder – Promega). Gels were run in 1 x TAE buffer at 100 V for 40 minutes.

When excising DNA, it is necessary to place the agarose gel under a UV light and behind a UV shield; this highlights the bands, allowing the bands to be cut out. Using a scalpel to cut

out the bands minimises the amount of gel taken that does not contain DNA. Tubes were weighed before, and then after the excised gel was added to find the weight of the samples. This was used to calculate the volume of gel dissolving buffer that was needed.

Open vectors, PCR products or DNA excised from agarose were purified using a Monarch® DNA Gel Extraction Kit following the supplier's instructions.

2.3.1.4 Ligation of Vector and Fragment

Typically, a 3:1 ratio (varied on occasion) was used along with T4 DNA ligase (Promega) when carrying out the ligation of vector, digested DNA fragments or PCR products. Ligations were usually incubated overnight alternating between 30°C and 10°C (112).

2.3.1.5 Transformation of DNA into Competent Cells

Chemically competent cells were prepared as described by Chang *et al*. (113) with the following modifications: The overnight culture was grown in 5 ml SOB and the dilution was also carried out using SOB rather than LB. The concentration of this dilution was also 1:5 to begin the next stage at an OD_{600} of 0.1. Following the subculturing and a 10-minute period of incubation in ice, the cells were centrifuged at 2500 x *g* at 4°C for 20 minutes. The pelleted cells were resuspended in 10 ml TB solution, before a further 10-minute incubation period in ice. Again, the cells were centrifuged at 2500 x *g* at 4°C for 10 minutes. The new pellets were then resuspended again in 1.86 ml TB solution and 140 µl DMSO 100%. There was a further 10 minute incubation period in ice before aliquoting 50 µl of cells into tubes to store rather than 5 ml as described (113).

2.3.1.6 Heat-Shock Transformation

Aliquots containing the appropriate competent cells (*E. coli* DH5α or *E. coli* S17-1 λ-pir) were thawed on ice before the ligation products were added at a ratio of 1:5. The mixture was then incubated on ice for 10 minutes before being placed in a heat block at 40-42°C for 1 minute, returned to ice for a further 10 minutes and then LB broth 950 µl was added to the cells. The new mixture was incubated at 37°C for 1-2 hours in a shaking incubator.

After incubation, the cells were added to a 1.5 ml tube before centrifugation at 12,000 x *g* for 1 minute. The supernatant was discarded, and 200 µl LB broth was used to resuspend the pelleted cells. The cells were then plated onto LB plates with appropriate antibiotics (plus x-gal where blue/white screening (114) is necessary). The plates were incubated at 37°C overnight.

2.3.2 Polymerase Chain Reaction

Polymerase chain reactions (PCR) were carried out using non-proofreading Go Taq® DNA polymerase (Promega). A standard 25 µl reaction consisted of 1 µl sample (boiled colony, gDNA etc.), 13.5 µl H_2O, 5 µl reaction buffer (Promega), 1 µl of each forward and reverse primers – 10 mM, 3 µl Mg^{2+} 25 mM, 0.4 µl dNTP's 10 mM and 0.1 µl Taq® polymerase (115).

PCR standard conditions were dependent on the size of the final product and the appropriate temperature for the primers used. The polymerase supplier's (Promega) instructions were followed when setting up the reactions. The primers used throughout the study are listed in Table 2.3.

Table 2.3: Primers used in this study (Restriction sites highlighted by underlining bold text)

Primer Name	Sequence (F: 5'-3') (R: 5'-3')	Restriction Enzyme	Source
RepA2-F	GTA**CTCGAG**CTGTTGCTCTATACAGG	XhoI	This Study
RepA2-R	CC**ACTAGT**TAA**CCCGGG**GTGAACAGGGCCTGGTG	SmaI / SpeI	This Study
CopB-F	CCA**CTCGAG**CGTACAGTCCAACTCGG	XhoI	This Study
CopB-R	GG**ACTAGT**CTT**CCCGGG**GGCACGTTTCGATGAGG	SmaI / SpeI	This Study
M13-R	TGTAAAACGACGGCCAGT	-	Promega©
luxC-R	CTACAACATCATAAAGGCC	-	Marco Grasso
pDM4-F	TAGCGGAGTGTATATCAAGC	-	Joanne Purves (Unpublished)

2.4 Detection of Luminescent colonies

A dark box was used to detect any light produced by the colonies on the antibiotic plates. Wasabi software was used in order to visualise the colonies. This was carried out to confirm the plasmid (containing *lux*) had been successfully inserted into the organism.

2.5 Conjugation

Cells were mated via conjugation as described by (116). Overnight cultures of the donor *E. coli* S17-1 λ–*pir* with the suicide plasmid were mixed in the ratios 1:1, 3:1, 5:1 and 9:1 with the recipient *Y. pseudotuberculosis* YpIII (Parent pYV$^+$, ΔII or ΔRR) in 1.5 ml tubes. The cells were pelleted at 12,000 x *g* for 1 minute and were resuspended in 1 ml YLB broth. The last step was repeated but with a resuspension in 30 µl YLB broth. These were spotted onto non-selective YLB plates. These were incubated for 24 hours at 37^{o}C before the cells were removed and resuspended in 0.2 ml YLB broth. This was then split into two and plated on YLB agar plates with appropriate antibiotics. These were incubated at 30^{o}C for several days or until single colonies were visible. Single colonies (particularly those producing light) were patched onto YLB agar plates with the appropriate antibiotics. The patch plates were also incubated at 30^{o}C until growth occurred.

2.6 Growth Curve

Any overnight cultures are measured in a spectrophotometer in order to calculate the volume needing to be added to the media to begin the curve at an OD of 0.1 (Using $C_1V_1=C_2V_2$). A ratio of 1:5 (Media: Container volume) was consistently used. Unless otherwise stated the media is YLB broth + the appropriate antibiotic.

A spectrophotometer is used every 30 minutes for between 6-10 hours to measure the OD_{600} of the culture.

3 Results

The aim was to identify whether QS plays a role in c*opA*/*copB* expression, and therefore pYV plasmid maintenance. *Lux*-based reporter fusions were constructed in order to measure the level of expression of the *copA* and c*opB* promoters both in the *Y. pseudotuberculosis* YPIII parent pYV^{+} strain, and mutants that have altered QS systems, either without the *ypsI*/*ytbI* ortholog or without the *ypsR*/*ytbR* ortholog.

During the construction of these fusions it was necessary to use pDM4.2, a suicide vector. This suicide vector forces the plasmid to integrate in the chromosome/plasmid in the desired organism via homologous recombination. *E. coli S17-1* possesses *λ-pir* which codes for the π protein, which is required to activate the origin of replication of pDM4.2 (116). When undergoing conjugation, the plasmid is left without the π protein required to undergo replication. This selective pressure forces the plasmid to either integrate into the *λ-pir* negative organism's pYV plasmid between the copA and copB promotors, or no replication can occur. Whereas *E. coli* DH5α (which had been transformed into for each other stage of the fusion construction) does not possess the *λ-pir* gene (and therefore cannot produce the π protein) and therefore pDM4.2 would never replicate within the organism (117). As a result, *E. coli* DH5α was used for the other plasmids but not the pDM4.2 derived ones.

3.1 Amplification of *CopA*/*CopB*

The first stage of this process involved extracting gDNA. The plasmid was extracted with the gDNA as the chromosome is large in size, causing them to precipitate with the plasmid still intact – this allowed the use of pYV as the template for the constructs. The promoter regions of *copA*/*copB* could then be amplified from the plasmid. gDNA extraction was carried out from an overnight *Y. pseudotuberculosis* YPIII Parent pYV+ culture grown at 30^{o}C. Agarose gel electrophoresis was performed to confirm the extracted material was of the quality required for use in future cloning steps. Agarose gel electrophoresis revealed that both gDNA samples were larger than the ladder as expected, proving chromosomal DNA was present. The first sample appears more refined due to a lower quantity of DNA thus less tangling of the fragments occurred and the second sample potentially being a larger quantity of DNA (Figure 3.1a). The concentration of the DNA was also determined using a nanodrop spectrophotometer and revealed that sample 1 and 2 contained 43 and 125 ng/µl respectively. PCR was then carried out, specifically on the pYV Plasmid Rep Operon, outlined in figure 3.2. Using the gDNA (and therefore pYV) as a template, PCR was performed to amplify the promoter regions of *copA* (primers RepA2-F and RepA2-R) and *copB* (copB-F and copB-R) (figure 3.2), and once complete the purified PCR products were analysed using agarose gel electrophoresis. Figure 3.1b reveals that the PCR worked as expected for *copA* and *copB* and amplified fragments of 149 bp (lanes 7-9) and 330 bp (lanes 2-4) respectively. Both 100 bp ladders (wells 6 and 11) did not separate as hoped for. However, this was not an issue as the 1 kb ladder worked as hoped. The appropriate bands (figure 3.1b - lanes 2-4, 8 and 9) were extracted from the gel, cleaned and re-analysed using agarose gel

electrophoresis, revealing that the extraction was successful and the fragments of 149 bp (*copA*) and 330 bp (*copB*) were suitable for use in the next step.

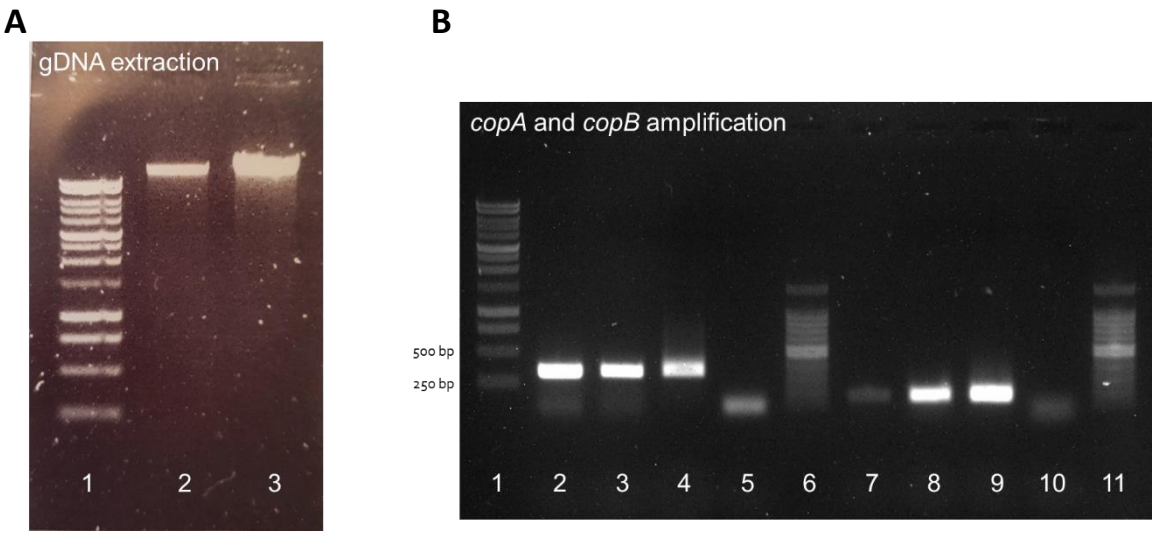

Figure 3.1: The prepared gDNA of *Y. pseudotuberculosis* YPIII PYV⁺ reveals the eligibility of the gDNA for use in the cloning process (A). In gel A: 1 kb ladder (1), and gDNA samples (2 & 3). The PCR products of the copA and copB promoter regions when using RepA2-F & RepA2-R primers for *copA*, and copB-F & copB-R for *copB* (B). This shows that the PCR worked correctly, with the correct fragments being formed. In gel B: 1 kb ladder (1), *copB* (2-4), *copA* (7-9), negative controls (5 & 10), and 100 bp ladders (6 & 11).

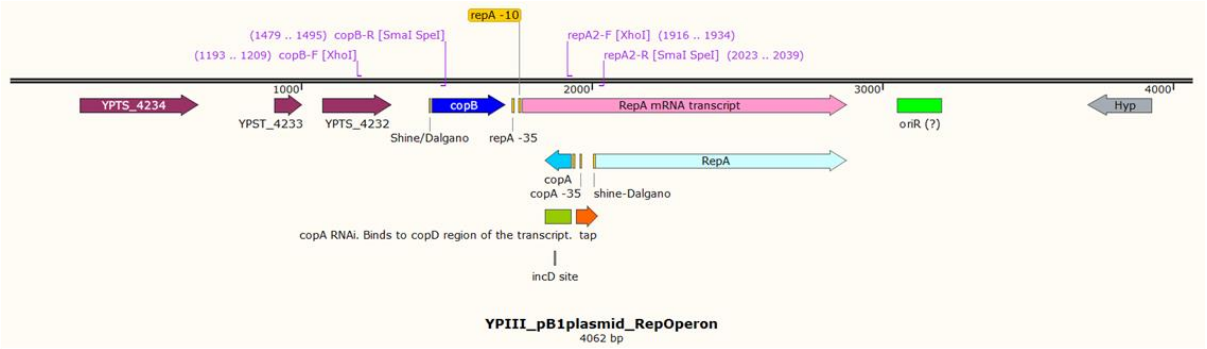

Figure 3.2: The pYV Rep Operon from *Y. pseudotuberculosis*, of which the *copA* and *copB* promoter regions were amplified. The purple labels indicate the locations of the primers (copB-F, copB-R, repA2-F, and repA2-R) used to amplify the regions.

3.2 Cloning of *copA*/*copB* into pGEM-T Easy

The next phase of the fusions involved cloning the amplified *copA* and *copB* fragments into the cloning vector pGEM-T Easy. A gel was run before carrying out a ligation to check both inserts, *copA* and *copB* (figure 3.3a). The expected size of the bands were 149 bp for *copA* and 330 bp for *copB*. The band at lane 2 is in between the 100 bp and 200 bp markers, suggesting that the *copA* fragment was as expected. Lane 3 can be seen between the 300 bp and 400 bp markers, also suggesting that the *copB* fragment was as expected. Both ladders (lanes 1 and 4) separated as hoped, though the 1 kb ladder was slightly distorted due to piercing of the well when adding the ladder. A ligation could then be carried out using the *copA*/*copB* fragments as inserts and pGEM-T Easy as a vector. The ligated products were then transformed into *E. coli DH5α* via heat-shock transformation. This strain allowed the use of blue-white screening – a mechanism that is based around β-galactosidase (a protein encoded by the *lacZ* gene) detection. X-gal allows for the detection of β-galactosidase activity, as the enzyme cleaves X-gal to form 5-bromo-4-chloro-indoxyl, which forms a blue insoluble pigment. When the *lacZα* gene is interrupted, for example via an insertion, its production of α-peptides is disrupted, preventing the formation of functional β-galactosidase. As a result, when X-gal is added, no cleaving takes place and therefore no colour change occurs (118). Blue-white screening was used to identify colonies containing pJd1::*copA*/pJd1::*copB*. PCR was carried out on these positive colonies to amplify the *copA* (using the primers repA2-F and M13-R) or *copB* (using the primers copB-F and M13-R) regions within the plasmid, and a gel was run to confirm the presence of the insertion. This gel (figure 3.3b) revealed *copA* and *copB* were present in the positive colonies that were tested – with the expected size of *copA* being 281 bp and the expected size of *copB* being 462 bp. Both sets of bands (5-7 and 10-14) were in the region of these anticipated sizes. The gel confirmed that *copA* and *copB* were successfully inserted in to pGEM to give pJd1::c*opA* and pJd1::*copB* (figure 3.4).

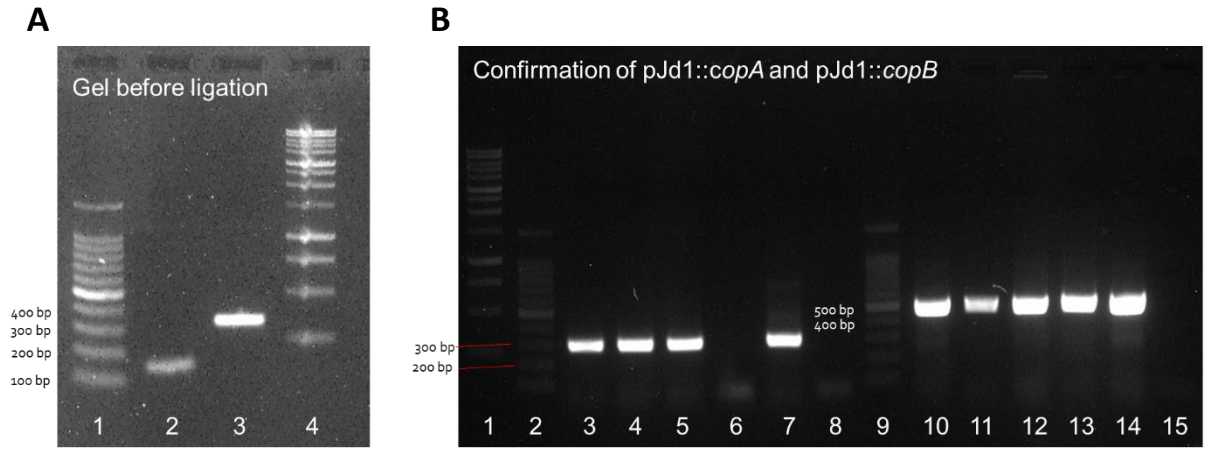

Figure 3.3: The gel before ligation reveals that the extracted material from previously is usable, and that the fragments have not been damaged or diluted in the process of extraction (A). In gel A: 100 bp ladder (1), *copA* (2), *copB* (3), and a 1 kb ladder (4). To confirm the creation of pJd1, PCR had to be carried out on seemingly positive colonies and the bands visualised to ensure the correct new fragment sizes are present (B). In gel B: 100 kb ladder (1), 100 bp ladders (2 & 9), copA (3-7), copB (10-14), negative controls (8 & 15).

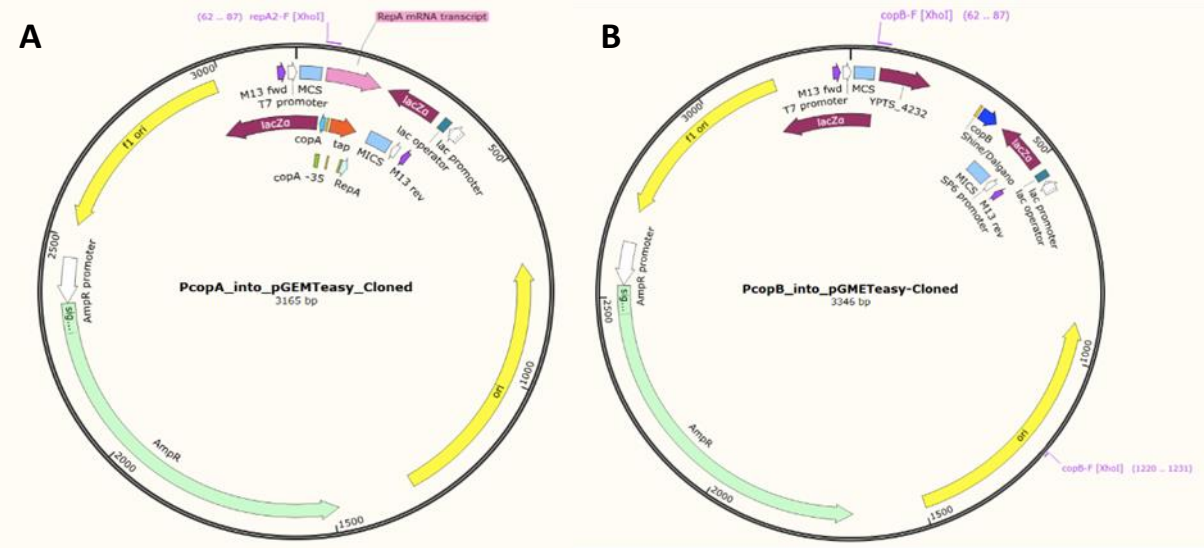

Figure 3.4: The plasmid maps of both pJd1::*copA* (A) and pJd1::*copB* (B). The purple labels indicate the sites of primers (repA2-F, copB-F, and M13 Fwd/M13 rev). The plasmids contain a mixture of both pGEM-T Easy and the amplified promoter regions of *copA* and *copB*.

3.3 Subcloning of the *luxCDABE* cassette

Step 3 in the fusion production was to combine both pJd1::*copA* and pJd1::*copB* with the *lux* cassette from pBlue-*lux* to produce the new plasmids pJd1:*copA*::*luxCDABE* and pJd1:*copB*::*luxCDABE*. The *lux* cassette component is the means of measuring expression in the final fusions, along with providing an easier screening method of using light. This works through the promoter (either from *copA* or *copB*) being activated, which switches leads to the expression of both QS components *luxI* and *luxR*, and also *luxCDABE*. This expression leads to bioluminescence of the cells. The greater the activity of the promoter, the greater the production of light. Minipreps were performed to isolate pJd1::*copA*, pJd1::*copB*, and pBlue-*lux* (a plasmid containing the *luxCDABE* cassette); following restriction of the newly isolated plasmids using the enzymes SmaI and SpeI, the resulting products were analysed on an agarose gel, before being extracted and cleaned. Once clean, the samples were again analysed on an agarose gel (figure 3.5a) which revealed that both vectors (pJd1::*copA* and pJd1::*copB*) ran at approximately 3 kb and matched to their expected sizes of 3,146 bp and 3,327 bp respectively. Similarly, the insert (*luxCDABE* cassette), digested from pBlue-*lux,* ran at approximately 6 kb, with the expected size being 5,864 bp. Following this check, ligations of both vectors and insert were carried out, leading to transformation into *E. coli DH5α*. Positive colonies were screened for light which was indicative of the successful insertion of *luxCDABE* into pJd1::*copA* and pJd1::*copB*, with the positive colonies being tested by performing PCR using repA2-F and luxC-R primers for copA, and copB-F and luxC-R for copB. The PCR products were then visualised on a gel (figure 3.5b). Figure 3.5b reveals the PCR worked as expected for both *copA* and *copB*, where the amplified fragments of 524 bp (lanes 3 & 4) and 705 bp (lanes 6 & 7), appear to be in the correct regions when compared to the ladders. As a result it was confirmed that *luxCDABE* had been successfully inserted into both

pJd1::*copA* and pJd1::*copB* to produce pJd1:*copA*::*luxCDABE* and pJd1:*copB*::*luxCDABE* (figure 3.6).

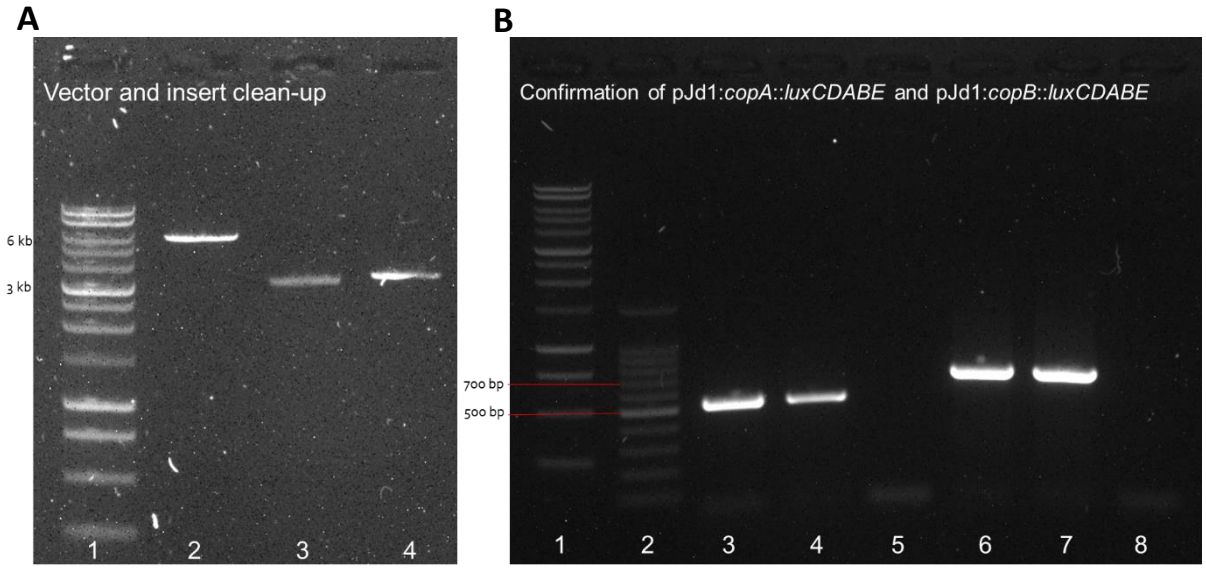

Figure 3.5: Samples of the extracted/cleaned vectors and insert were visualised to ensure the newly digested fragments were still of a good quality, and that the clean-up of the vectors had been a success before using them in the next stage of the cloning process (A). In gel A: 1 kb ladder (1), *lux* (2), pJd1::*copA* (3), and pJd1::*copB* (4). PCR was carried out on seemingly positive colonies, with the results being visualised to reveal whether the fragment sizes are as anticipated, confirming the creation of the new plasmids (B). In gel B: 1 kb ladder (1), 100 bp ladder (2), pJd1:*copA*::*luxCDABE* (3 & 4), pJd1:*copB*::*luxCDABE* (6 & 7), and negative controls (5 & 8).

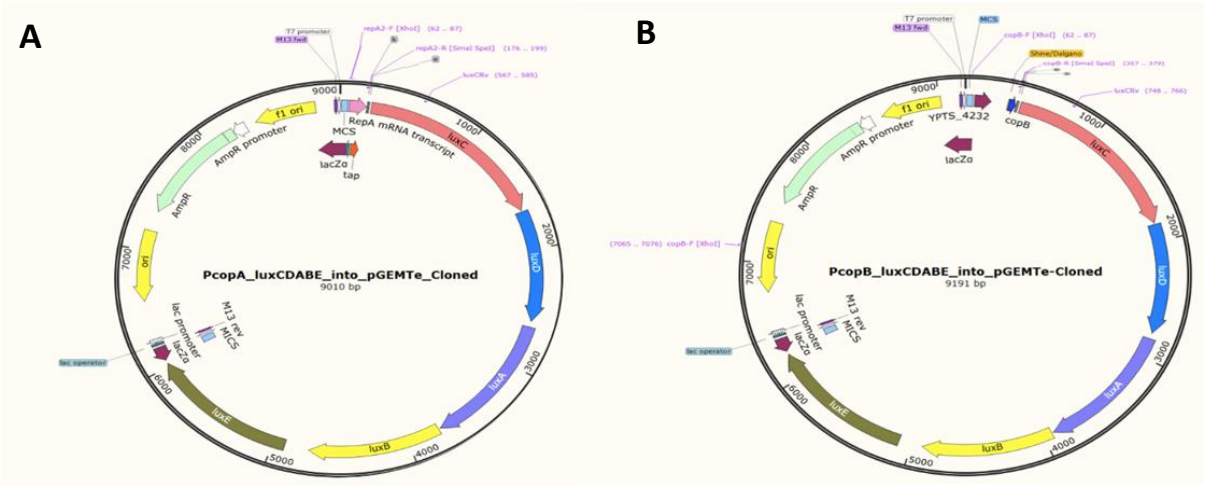

Figure 3.6: The plasmid maps of pJd1:*copA*::*luxCDABE* (A) and pJd1:*copB*::*luxCDABE* (B). The purple labels indicate the use of primers in these locations. Among these are the M13 primers, that are instead indicated with labels inside the plasmid maps. The plasmids consist of pGEM-T Easy, the amplified promoter regions of *copA* and *copB*, and a *lux* cassette from pBlue*lux*.

3.4 Subcloning of *copA*::*luxCDABE*/*copB*::*luxCDABE* into pDM4.2

It was then necessary to use pDM4.2 as a new vector, with the *copA*/*copB* and *luxCDABE* portions of pJd1:*copA*::*luxCDABE* and pJd1:*copB*::*luxCDABE* being inserted. pDM4.2 was chosen for its properties as a suicide vector. Restriction digests were performed on pDM4.2, pJd1:*copA*::*luxCDABE*, and pJd1:*copB*::*luxCDABE* using SpeI and XhoI sites, and agarose gel electrophoresis was carried out on the digested products. Gel extraction and ligation were then performed using pDM4.2 as a vector and the digest products *copA*::*luxCDABE* and *copB*::*luxCDABE* as the inserts. The ligations were heat-shock transformed, into *E. coli* S17-1 λ-pir as it encodes the π protein required for the replication of pDM4.2. Once the transformants grew, they were screened using a dark box to identify bioluminescent colonies, and PCR. Figure 3.7a reveals following PCR screening (using the primers luxC-R and pDM4-F) colonies contain pJd2:*copA*::*luxCDABE* with the expected band size being 559 bp (lanes 2-5). Each of the bands were in the region of this anticipated size. Similarly, figure 3.7b reveals following screening via PCR (using the primers luxC-R and pDM4-F) the other screened colonies contain pJd2:*copB*::*luxCDABE* with the expected size of these bands being 740 bp (lanes 2-5). This confirmed that pJd1:*copA*::*luxCDABE* and pJd1:*copB*::*luxCDABE* had both been successfully ligated into pDM4.2 to produce pJd2:*copA*::*luxCDABE* and pJd2:*copB*::*luxCDABE*.

Conjugations were carried out using pJd2:*copA*::*luxCDABE* and pJd2:*copB*::*luxCDABE* with *Y. pseudotuberculosis* YPIII Parent pYV^{+}, *Y. pseudotuberculosis* YPIII ΔRR, and *Y. pseudotuberculosis* YPIII ΔII (the genetic backgrounds of these strains can be found in table 2.1). The conjugations were screened using both light detection and PCR to confirm the presence of the fusions.

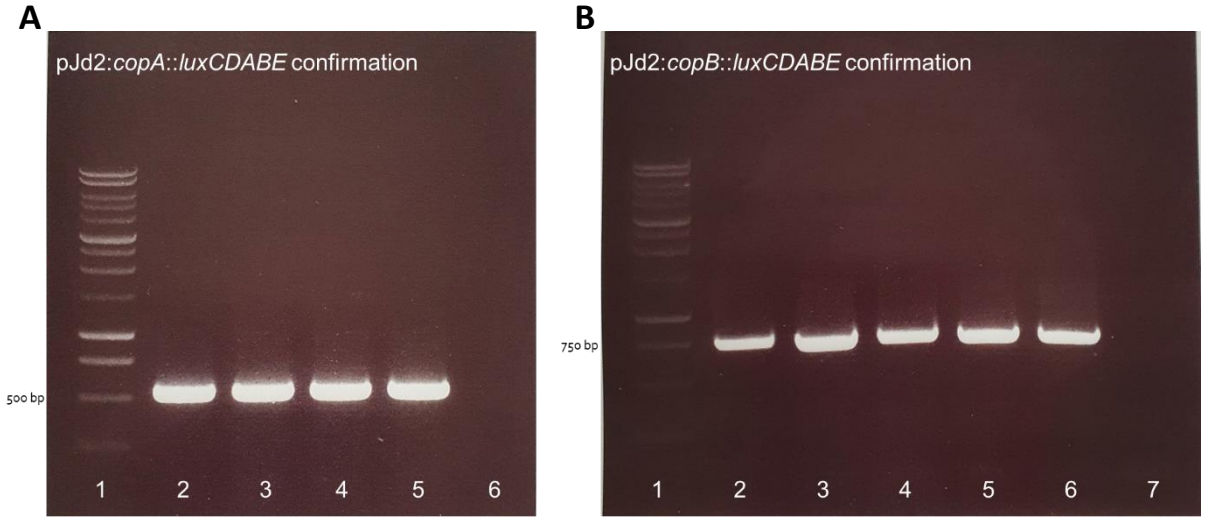

Figure 3.7: PCR was carried out on light positive colonies containing pJd2:*copA*::*luxCDABE* to ensure the fusion was correctly created (A). In gel A: 1 kb ladder (1), *copA* (2-5), and a negative control (6). Similarly, PCR was carried out on the pJd2:*copB*::*luxCDABE* based fusion to ensure it was as hoped for (B). In gel B: 1 kb ladder (1), *copB* (2-6), and a negative control (7).

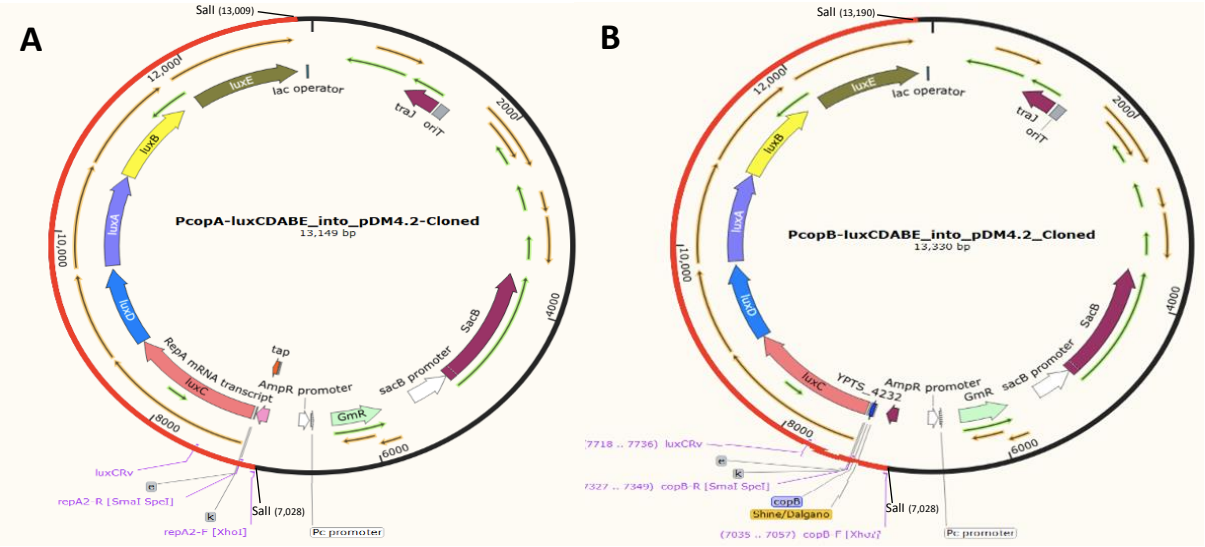

Figure 3.8: The plasmid maps of pJd2:*copA*::*luxCDABE* (A) and pJd2:*copB*::*luxCDABE* (B). Primer locations are highlighted in purple text. These plasmids consist mostly of pDM4.2, along with large segments of the previously constructed pJd1:*copA*::*luxCDABE* and pJd1:*copB*::*luxCDABE*.

associated with using a single restriction site, the first being self-ligation of the insert/vector. Another risk is orientation – if the insert and vector are ligated successfully, there is a risk that the insert may be in the incorrect orientation and thus not function correctly. A way to prevent this was to dephosphorylate the vector before carrying out the ligation, this prevents self-ligation occurring. The digested products were visualised on a gel. This process had to be repeated several times, with a few variations in how pHG327 was handled. The growth media was changed to Brain Heart Infusion (BHI) agar, which is richer in nutrients, to encourage greater cell growth following a lack of visual bands when carrying out gels. Once successful, a ligation was carried out with an altered ratio of 5:1 with pJd2:*copA*::*luxCDABE* and pJd2:*copB*::*luxCDABE* as the inserts and pHG327 as the vector. Previous ligations had been carried out using high copy number plasmids, as such the ratio was increased to improve the chances of a successful ligation when using a low copy number plasmid. A transformation was then undertaken using *E. coli* S17-1 λ–pir and the plates were screened for potential positive colonies using a combination of light detection and PCR. Figure 3.9 reveals the process was unsuccessful, with the expected band sizes being approximately 6 kb and 3.4 kb (wells 1-4). Both bands were above the expected sizes, along with the presence of an unexpected third band, which may be the result of a partial digest. As a result the construction of pJd3:*copA*::*luxCDABE* and pJd3:*copB*::*luxCDABE* could not be confirmed and will need repeating when possible to do so.

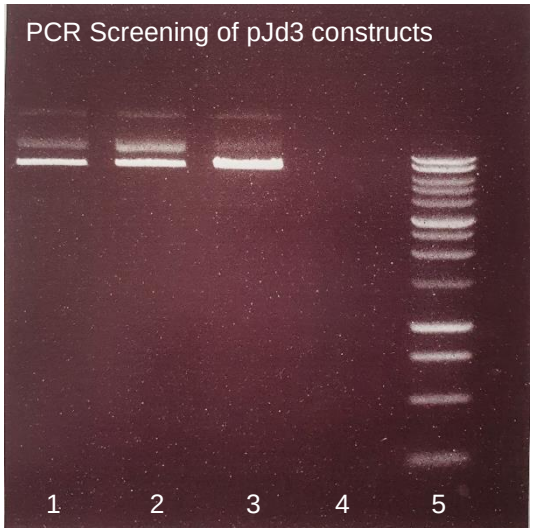

Figure 3.9: PCR was carried out on light colonies, and in the case of *copA*, colonies that sufficiently grew, following a lack of light consistently in these constructs. In this gel: pJd3:*copB*::*luxCDABE* (1 & 2), pJd3:*copA*::*luxCDABE* (3 & 4), and a 1 kb ladder (5). It was hoped that this gel would confirm the construction of both plasmids.

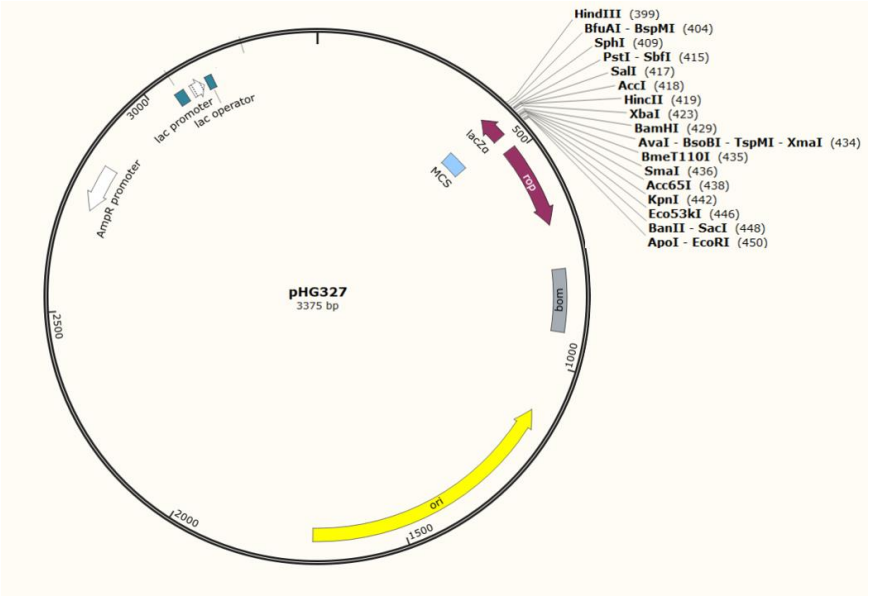

Figure 3.10: A map of the cloning vector pHG327, including each restriction site it possesses. The group of these sites is located on the Multi-cloning site (MCS), to ease the digestion process when integrating an insert into the vector.

4 Discussion

The study aimed to learn whether QS plays a role in *copA*/*copB* and therefore pYV plasmid maintenance. This was attempted through the construction of *lux*-based reporter fusions, in order to measure the level of expression of *copA* and *copB* promoters when the QS synthases, ypsI/ytbI or ypsR/ytbR, are removed from the quorum sensing system within *Y. pseudotuberculosis*. These were previously removed through deletions as described by Atkinson *et al*. (97).

Amplification of *copA*/*copB* promoters

The processes involved in extracting gDNA from the parent culture of *Y. pseudotuberculosis* YPIII PYV^{+} went smoothly, as did the amplification of both promoter regions of *copA* and c*opB*. The only mishap was a lack of separation in the 100 bp ladders, which did not impact on this stage due to a 1 kb ladder also being used.

Cloning of *copA*/*copB* promoters into pGEM-T Easy

At the second stage of the fusion production, the amplified regions of *copA*/*copB* were inserted into the vector pGEM-T Easy. Most of the process was straight forward with no errors. However, there was one minor issue when it came to the gel, whereby the gel was pierced by the pipette tip when adding the 1 kb ladder (figure 3.3a) which created a slightly deformed ladder, though this did not impact on the ability to read the gel. The only other issue with this stage of the fusion construction was the blue-white screening. The screening worked effectively with *copB* as the larger insertion disrupted the *lacZ* to a larger extent, preventing the production of effective α-peptides, in order to produce β-galactosidase. However, the c*opA* insert is smaller in size and as a result the disruption to the *lacZ* gene sequence is minimal. This led to some colouration in the colonies regardless of whether the insert was present or not. The problem was solved by continuing to target the white or the palest blue colonies formed, suggesting there is only a limited production/inactivation of β-galactosidase, as a result of abnormal or very few α-peptides being produced (118).

Subcloning of *luxCDABE* to create the reporter fusions

The next step involved the insertion of the pBlue*lux luxCDABE* cassette into pJd1::*copA* and pJd1::*copB*. This was necessary to measure the levels of expression within the fusions, along with the use of light as a method of screening for positive colonies. There were no issues within this process, and each step worked as expected.

Subcloning of *copA*::*luxCDABE*/*copB*::*luxCDABE* into pDM4.2

At this stage, the aim was to produce pJd2:*copA*::*luxCDABE* and pJd2:*copB*::*luxCDABE*, which possess the qualities of a suicide plasmid due to the involvement of pDM4.2. These plasmids were then integrated into *Y. pseudotuberculosis* YPIII Parent pYV^{+}, and the mutants *Y. pseudotuberculosis* YPIII ΔRR, and *Y. pseudotuberculosis* YPIII ΔII. Several issues arose throughout this step, all of which were during the process of conjugation and not the creation of the fusions themselves. Several repeats were necessary for most of the constructs. The first of these reasons was a lawn of bacterial growth over the conjugation plates, rather than the desired individual colonies. The likely cause of this is too large a quantity of viable cells, causing exponential growth of cells, leading to the lawn of bacteria. As a result, the ratio of 9:1 (the largest ratio that had been already carried out previously in the study) was focussed on for these constructs to reduce the number of viable cells and as a result dilute the contents of the plates – this was successful after a few attempts. The next issue was a lack of light being picked up for the *copA*-based constructs. After attempting to alter the method in a variety of ways including change in ratio, volume etc. it was realised that the *copA*-based fusions are likely to have produced light very early in their growth and as a result this light production was usually missed. It is likely that the early light production is down to rate of growth of the organism. Light production occurs during the exponential growth phase of the bacteria's typical growth curve (119; 120). This difference in growth rate could be attributed to the difference in metabolic load between the two different fusions. As the *copB* fusion is larger in size, the bacterium carries a slightly higher metabolic load, whereas the *copA* fusion is smaller, slightly reducing the metabolic load. It has been suggested that a higher metabolic load/larger plasmid leads to a slower growth rate in otherwise identical bacteria (67). To counter this, patch plates were created so that PCR could be used on several different colonies rather than relying on light. Screening via PCR is advantageous because it reveals whether the colonies contain specific components of the fusions, rather than relying on just a functioning *lux* cassette. The introduction of the patch plates allowed for repeats of PCR if necessary, along with increasing light visibility due to the higher quantity of bacteria.

Subcloning of the reporter fusions into pHG327

To create the alternative fusions, the reporter regions (*lux* and *copA*/*B*) of pJd2:*copA*::*luxCDABE* and pJd2:c*opB*::*luxCDABE* were inserted into pHG327. The intention of this alternative set of fusions is to transform the plasmid directly into *Y. pseudotuberculosis* cells, compared to forcing integration via a suicide plasmid. pHG327 was the chosen vector, as it possesses an extremely low plasmid copy number. Each additional copy leads to a greater production of light, therefore decreasing the accuracy when measuring expression using *luxCDABE* as a marker. Although not perfect, the low copy number should more accurately reflect the expression from the native promoters, which may not be possible with the other fusions. There may be issues with the pDM4.2 fusions as this method does not always lead to successful integration via homologous recombination due to this needing to occur between the copA and copB promoters, with only a single copy of the plasmid. The pHG327 method removes the struggle of integrating the reporters via homologous recombination.

There were consistent issues with this process, starting with the struggle to visualise a band of pHG327 on a gel following a digestion. This issue is common with low copy number plasmids due to a limited quantity of DNA to work with. To try to fix this problem, the growth media for *E. coli* pHG327 was changed from LB agar to BHI agar to increase the nutrients available, therefore encouraging greater growth and as a result gain more genetic material to work with. Other methods of increasing the plasmid yield could have included increasing the volume of the starting culture, subculturing from a single colony, or attempting a variety of different growth conditions such as length of time. The chosen method seemed to work and resulted in the production of bands on a gel. A ligation and transformation were carried out, with the resulting colonies being screened via PCR. Despite the change in media, the subcloning process failed. Bands were visualised as hoped for, but the sizes of these bands were not what was expected (figure 3.9). At this point, the project had to pause, preventing a repeat of this process.

Research plans for further work

The plan was to carry out Bioluminescence assays using a Tecan Spark® microplate reader with SparkControl software on the fusions to find any differences in level of expression of *copA*/*copB*, in order to gain an understanding of the role of QS in plasmid maintenance. The assays would consist of each fusion in the parent and QS mutants and would allow for comparison to identify what components of the QS system are important in plasmid maintenance. It would highlight whether there is a difference in *copA* and *copB* expression, along with identifying if the I or R orthologs play a significant role in the process. If downregulation occurs in the mutants compared to the parent strain, it could be suggested that QS has a positive regulatory role in the *copA* and/or *copB* promoters (110). It has previously been found that when not bound to autoinducers (AI), *LuxR* proteins are rapidly degraded, presumably to prevent bacteria from short-circuiting their QS systems (94). However, if upregulation of expression occurs, it may be that the QS system still has an important role in plasmid maintenance, but a repressive role. The assays ultimately would identify or further prove the relationship between each component of the pYV plasmid maintenance system. It was also intended to produce a set of pHG327 based fusions. These would also have been tested with Tecan assays to act as a comparison to the suicide plasmid-based fusions. While the light output/levels of expression may differ between the two sets of fusions, if the trend in data is identical it would suggest the results are accurate, without the possibility of inaccuracy when two different approaches reach the same conclusion.

If there was a mutant that stood out in terms of results, then this information could be taken further into producing single *Y. pseudotuberculosis* ΔI or ΔR to identify which individual component of each pairing (for example *yspI* vs *ytbI*, or *yspR* vs *ytbR*) has the greater impact on QS, or if there even is a difference within the pairs.

To also further test the theory that QS plays a role in *Yersinia* plasmid maintenance, it would be interesting to follow up the Tecan assays with using a variety of QS inhibiting compounds to see if this influences the expression of *copA* and c*opB*. An example of this could be

flavanones, such as naringin, neohesperidin, and hesperidin, all of which have been seen to possess anti-QS characteristics. The study by Truchado e*t al.* (121) on these compounds revealed orange extract's main flavanone components exert a QS inhibitory effect on *Y. enterocolitica*. It was proven that the AHL level was reduced dramatically when introducing these flavanones. The impacts also continued in biofilm formation and motility, both of which were reduced significantly. This is supported by another previous study based on *Pseudomonas aeruginosa* where similar effects were observed on the organism's QS mechanisms (122). If the levels of expression changed as a result of these compounds, it would suggest that either c*opA*, *copB*, or both, are influenced by QS.

This work could be followed up by using the a*iiA* gene, which encodes for an autoinducer inactivating enzyme (123). This gene could be inserted into the existing fusions to degrade AHLs produced by the QS system. The new fusions could be used in the same way that both ΔII and ΔRR *Y. pseudotuberculosis* mutants were, preventing the QS system working as it normally would and discovering whether the expression of *copA* and c*opB* is affected. However, this method may be better as it does not require the removal of either I/R ortholog. There is potential risk that any component in these orthologs may have an additional role that we are unaware of. With the *aiiA* gene approach, this risk factor is removed.

Another potential direction could be to use the *aiiA* gene in the fusions, but measure plasmid loss rather than expression of *copA*/*copB*. Plasmid loss could be assessed using the *luxCDABE* cassette as a marker of plasmid presence, meaning those colonies without light have lost the plasmid. While the data in this case would be related to plasmid loss, the results would have implications on plasmid maintenance if there was a difference between the fusions containing the a*iiA* gene and those such as pJd2:*copA*::*luxCDABE* and pJd2:*copB*::*luxCDABE*, within the parent strain of *Y. pseudotuberculosis*.

A possible target to look into for the future could be the ParDE Toxin-Antitoxin system. Whilst not extensively characterised in *Yersinia*, it was discovered that there are ParDE homologues on pCD1 in *Yersinia pestis* along with a presence on the chromosome of *Y. enterocolitica* (124). The system is known to contribute to stable maintenance of the RK2 plasmid within *Escherichia coli* and several related bacteria (125; 126), along with promoting biofilm formation (126). This information leads me to believe the system is worth further investigation within *Yersinia*. Biofilm formation has close links to QS, and as ParDE has links to both biofilm formation and plasmid maintenance within *E. coli* (which has several similar characteristics to *Yersinia*) QS and this system may overlap. However, ParDE and its functions within *Yersinia* are unknown and as such the system would need characterisation before moving on to investigate possible ties between the TA system, QS and plasmid maintenance.

Conclusion

In conclusion, whilst the data for the constructs could not be gathered at this point, strides in the right direction were made. The first set of fusions were successfully created, allowing them to be used to collect data when it is possible. pJd3:*copA*::*luxCDABE* and pJd3:c*opB*::*luxCDABE* were not finished and as a result will need to be created upon

continuation of the project. It will be at this point, when both sets of fusions can be compared and the data can be sufficiently analysed.

References

1. Sabina, Y., Rahman, A., Ray, R. and Montet, D., 2011. Yersinia enterocolitica: Mode of Transmission, Molecular Insights of Virulence, and Pathogenesis of Infection. *Journal of Pathogens*, 2011: 429069
2. Le Guern AS, Savin C, Angermeier H, Brémont S, Clermont D, Mühle E, et al. sp. nov.,. *Int J Syst Evol Microbiol*. 2020;70(10):5363-72.
3. Brubaker, R. R. 1991. Factors promoting acute and chronic diseases caused by yersiniae. *Clin Microbiol Rev*, 4, 309-24.
4. Amphlett, A. 2016. Far East Scarlet-Like Fever: A Review of the Epidemiology, Symptomatology, and Role of Superantigenic Toxin: Yersinia pseudotuberculosis-Derived Mitogen A. *Open Forum Infect Dis*, 3, ofv202.
5. EFSA Journal, 2007. Monitoring and identification of human enteropathogenic Yersinia spp. - Scientific Opinion of the Panel on Biological Hazards. 5(12), p.595.
6. Mandell, G. L., Bennett, J. E., Dolin, R. Mandell, Douglas, and Bennett's Principles and Practice of Infectious Diseases Seventh Edition, vol 2, 2009, p.2943-2952.
7. Aziz, M., Waheed, A. & Yelamanchili, V. S. 2020. Yersinia Enterocolitica. StatPearls Publishing LLC.
8. Who.int. 2016. Plague. [online] Available at: <https://www.who.int/news-room/fact-sheets/detail/plague>
9. Bertherat, E. Plague around the world in 2019/La peste dans le monde en 2019. *Weekly Epidemiological Record*, vol. 94, no. 25, 2019, p. 289+.
10. Zimbler DL, Schroeder JA, Eddy JL, Lathem WW. Early emergence of Yersinia pestis as a severe respiratory pathogen. *Nat Commun*. 2015; 6:7487.
11. Morelli G, Song Y, Mazzoni CJ, Eppinger M, Roumagnac P, Wagner DM, et al. Yersinia pestis genome sequencing identifies patterns of global phylogenetic diversity. Nat Genet. 2010;42(12):1140-3.
12. Who.int. 2017. Plague – Madagascar [online] available at <https://www.who.int/csr/don/27-november-2017-plague-madagascar/en/>
13. Raoult, D., Mouffok, N., Bitam, I., Piarroux, R. & Drancourt, M. 2013. Plague: history and contemporary analysis. *J Infect*, 66, 18-26.
14. Achtman, M., Zurth, K., Morelli, G., Torrea, G., Guiyoule, A. and Carniel, E., 1999. Yersinia pestis, the cause of plague, is a recently emerged clone of Yersinia pseudotuberculosis. *Proceedings of the National Academy of Sciences*, 96(24), pp.14043-14048.
15. Savin, C., Criscuolo, A., Guglielmini, J., Le Guern, A. S., Carniel, E., Pizarro-Cerdá, J. & Brisse, S. 2019. Genus-wide Yersinia core-genome multilocus sequence typing for species identification and strain characterization. *Microb Genom*, 5.
16. Chain, P. S., Carniel, E., Larimer, F. W., Lamerdin, J., Stoutland, P. O., Regala, W. M., Georgescu, A. M., Vergez, L. M., Land, M. L., Motin, V. L., Brubaker, R. R., Fowler, J., Hinnebusch, J., Marceau, M., Medigue, C., Simonet, M., Chenal-Francisque, V., Souza, B., Dacheux, D., Elliott, J. M., Derbise, A., Hauser, L. J. & Garcia, E. 2004. Insights into the evolution of Yersinia pestis through whole-genome comparison with Yersinia pseudotuberculosis. *Proc Natl Acad Sci U S A*, 101, 13826-31.

17. Pizarro-Cerdá, J. & Cossart, P. 2006. Bacterial adhesion and entry into host cells. *Cell*, 124, 715-27.
18. Chauhan, N., Wrobel, A., Skurnik, M. & Leo, J. C. 2016. Yersinia adhesins: An arsenal for infection. *Proteomics Clin Appl*, 10, 949-963.
19. Mühlenkamp, M., Oberhettinger, P., Leo, J. C., Linke, D. & Schütz, M. S. 2015. Yersinia adhesin A (YadA)--beauty & beast. *Int J Med Microbiol*, 305, 252-8.
20. Hoiczyk, E., Roggenkamp, A., Reichenbecher, M., Lupas, A. & Heesemann, J. 2000. Structure and sequence analysis of Yersinia YadA and Moraxella UspAs reveal a novel class of adhesins. *EMBO J*, 19, 5989-99.
21. Mikula, K. M., Kolodziejczyk, R. & Goldman, A. 2012. Yersinia infection tools-characterization of structure and function of adhesins. *Front Cell Infect Microbiol*, 2, 169.
22. Clark, M. A., Hirst, B. H. & Jepson, M. A. 1998. M-cell surface beta1 integrin expression and invasin-mediated targeting of Yersinia pseudotuberculosis to mouse Peyer's patch M cells. *Infect Immun*, 66, 1237-43.
23. Hamburger, Z. A., Brown, M. S., Isberg, R. R. & Bjorkman, P. J. 1999. Crystal structure of invasin: a bacterial integrin-binding protein. *Science*, 286, 291-5.
24. Miller, V. L., Bliska, J. B. & Falkow, S. 1990. Nucleotide sequence of the Yersinia enterocolitica ail gene and characterization of the Ail protein product. *J Bacteriol*, 172, 1062-9.
25. Atkinson, S. and Williams, P., 2016. Yersinia virulence factors - a sophisticated arsenal for combating host defences. *F1000Research*, 5, p.1370.
26. Snellings, N. J., Popek, M. & Lindler, L. E. 2001. Complete DNA sequence of Yersinia enterocolitica serotype 0:8 low-calcium-response plasmid reveals a new virulence plasmid-associated replicon. *Infect Immun*, 69, 4627-38.
27. Cornelis, G. R., Boland, A., Boyd, A. P., Geuijen, C., Iriarte, M., Neyt, C., Sory, M. P. & Stainier, I. 1998. The virulence plasmid of Yersinia, an antihost genome. *Microbiol Mol Biol Rev*, 62, 1315-52.
28. Stainier, I. & Cornelis, G. R. 1998. The Yop virulon of Yersinia: a bacterial weapon to kill host cells. *Clin Microbiol Infect*, 4, 673-676.
29. Ch'ng, S. L., Octavia, S., Xia, Q., Duong, A., Tanaka, M. M., Fukushima, H. & Lan, R. 2011. Population structure and evolution of pathogenicity of Yersinia pseudotuberculosis. *Appl Environ Microbiol*, 77, 768-75.
30. Simonet, M., Richard, S. & Berche, P. 1990. Electron microscopic evidence for in vivo extracellular localization of Yersinia pseudotuberculosis harboring the pYV plasmid. *Infect Immun*, 58, 841-5.
31. Portnoy, D. A. & Falkow, S. 1981. Virulence-associated plasmids from Yersinia enterocolitica and Yersinia pestis. *J Bacteriol*, 148, 877-83.
32. Coburn, B., Sekirov, I. & Finlay, B. B. 2007. Type III secretion systems and disease. *Clin Microbiol Rev*, 20, 535-49.
33. Dewoody, R. S., Merritt, P. M. & Marketon, M. M. 2013. Regulation of the Yersinia type III secretion system: traffic control. *Front Cell Infect Microbiol*, 3, 4.

34. Portaliou, A. G., Tsolis, K. C., Loos, M. S., Zorzini, V. & Economou, A. 2016. Type III Secretion: Building and Operating a Remarkable Nanomachine. *Trends Biochem Sci*, 41, 175-189.
35. Schraidt, O. & Marlovits, T. C. 2011. Three-dimensional model of Salmonella's needle complex at subnanometer resolution. *Science*, 331, 1192-5.
36. Diepold, A., Kudryashev, M., Delalez, N. J., Berry, R. M. & Armitage, J. P. 2015. Composition, formation, and regulation of the cytosolic c-ring, a dynamic component of the type III secretion injectisome. *PLoS Biol*, 13, e1002039.
37. Diepold, A., Wiesand, U. & Cornelis, G. R. 2011. The assembly of the export apparatus (YscR,S,T,U,V) of the Yersinia type III secretion apparatus occurs independently of other structural components and involves the formation of an YscV oligomer. *Mol Microbiol*, 82, 502-14.
38. Diepold, A., Wiesand, U., Amstutz, M. & Cornelis, G. R. 2012. Assembly of the Yersinia injectisome: the missing pieces. *Mol Microbiol*, 85, 878-92.
39. Payne, P. L. & Straley, S. C. 1999. YscP of Yersinia pestis is a secreted component of the Yop secretion system. *J Bacteriol*, 181, 2852-62.
40. Payne, P. L. & Straley, S. C. 1998. YscO of Yersinia pestis is a mobile core component of the Yop secretion system. *J Bacteriol*, 180, 3882-90.
41. Cornelis, G. R. 2002. The Yersinia YSC-YOP 'Type III' Weaponry. Nature Review | *Molecular Cell Biology*, 3.
42. Pan, N. J., Brady, M. J., Leong, J. M. & Goguen, J. D. 2009. Targeting type III secretion in Yersinia pestis. *Antimicrob Agents Chemother*, 53, 385-92.
43. Edqvist, P. J., Aili, M., Liu, J. & Francis, M. S. 2007. Minimal YopB and YopD translocator secretion by Yersinia is sufficient for Yop-effector delivery into target cells. *Microbes Infect*, 9, 224-33.
44. Chaudhury, S., De Azevedo Souza, C., Plano, G. V. & De Guzman, R. N. 2015. The LcrG Tip Chaperone Protein of the Yersinia pestis Type III Secretion System Is Partially Folded. *J Mol Biol*, 427, 3096-109.
45. Perry, R. D., Straley, S. C., Fetherston, J. D., Rose, D. J., Gregor, J. & Blattner, F. R. 1998. DNA sequencing and analysis of the low-Ca2+-response plasmid pCD1 of Yersinia pestis KIM5. *Infect Immun*, 66, 4611-23.
46. Dittmann, S., Schmid, A., Richter, S., Trülzsch, K., Heesemann, J. & Wilharm, G. 2007. The Yersinia enterocolitica type three secretion chaperone SycO is integrated into the Yop regulatory network and binds to the Yop secretion protein YscM1. *BMC Microbiol*, 7, 67.
47. Burkinshaw, B. J. & Strynadka, N. C. 2014. Assembly and structure of the T3SS. *Biochim Biophys Acta*, 1843, 1649-63.
48. Galindo, C. L., Rosenzweig, J. A., Kirtley, M. L. & Chopra, A. K. 2011. Pathogenesis of Y. enterocolitica and Y. pseudotuberculosis in Human Yersiniosis. *J Pathog*, 2011, 182051.
49. Matsumoto, H. & Young, G. M. 2009. Translocated effectors of Yersinia. *Curr Opin Microbiol*, 12, 94-100.

50. Aepfelbacher, M., Trasak, C., Wilharm, G., Wiedemann, A., Trulzsch, K., Krauss, K., Gierschik, P. & Heesemann, J. 2003. Characterization of YopT effects on Rho GTPases in Yersinia enterocolitica-infected cells. *J Biol Chem*, 278, 33217-23.
51. Schmidt, G. 2011. Yersinia enterocolitica outer protein T (YopT). *Eur J Cell Biol*, 90, 955-8.
52. Boland, A. & Cornelis, G. R. 1998. Role of YopP in suppression of tumor necrosis factor alpha release by macrophages during Yersinia infection. *Infect Immun*, 66, 1878-84.
53. Schoberle, T. J., Chung, L. K., Mcphee, J. B., Bogin, B. & Bliska, J. B. 2016. Uncovering an Important Role for YopJ in the Inhibition of Caspase-1 in Activated Macrophages and Promoting Yersinia pseudotuberculosis Virulence. *Infect Immun*, 84, 1062-1072.
54. Bertrand, J., Rüther, C., Scharnert, J., Niedermeier, M., Schmidt, A. & Pap, T. 2011. The bacterial effector protein YopM is a self delivering immune therapeutic agent that reduces inflammation in rheumatoid arthritis. *Annals of the Rheumatic Diseases*.
55. Ratner, D., Orning, M. P., Proulx, M. K., Wang, D., Gavrilin, M. A., Wewers, M. D., Alnemri, E. S., Johnson, P. F., Lee, B., Mecsas, J., Kayagaki, N., Goguen, J. D. & Lien, E. 2016. The Yersinia pestis Effector YopM Inhibits Pyrin Inflammasome Activation. *PLoS Pathog*, 12, e1006035.
56. Chung, L. K., Park, Y. H., Zheng, Y., Brodsky, I. E., Hearing, P., Kastner, D. L., Chae, J. J. & Bliska, J. B. 2016. The Yersinia Virulence Factor YopM Hijacks Host Kinases to Inhibit Type III Effector-Triggered Activation of the Pyrin Inflammasome. *Cell Host Microbe*, 20, 296-306.
57. Lähteenmäki, K., Kukkonen, M. & Korhonen, T. K. 2001. The Pla surface protease/adhesin of Yersinia pestis mediates bacterial invasion into human endothelial cells. *FEBS Lett*, 504, 69-72.
58. Patzer, S. I., Albrecht, R., Braun, V. & Zeth, K. 2012. Structural and mechanistic studies of pesticin, a bacterial homolog of phage lysozymes. *J Biol Chem*, 287, 23381-96.
59. Hinnebusch, B. J., Rudolph, A. E., Cherepanov, P., Dixon, J. E., Schwan, T. G. & Forsberg, A. 2002. Role of Yersinia murine toxin in survival of Yersinia pestis in the midgut of the flea vector. *Science,* 296, 733-5.
60. Sengupta, M. & Austin, S. 2011. Prevalence and significance of plasmid maintenance functions in the virulence plasmids of pathogenic bacteria. *Infect Immun*, 79, 2502-9.
61. Million-Weaver, S. & Camps, M. 2014. Mechanisms of plasmid segregation: have multicopy plasmids been overlooked? *Plasmid*, 75, 27-36.
62. Schumacher, M. A. 2012. Bacterial plasmid partition machinery: a minimalist approach to survival. *Curr Opin Struct Biol*, 22, 72-9.
63. Ebersbach, G. & Gerdes, K. 2005. Plasmid segregation mechanisms. *Annu Rev Genet*, 39, 453-79.
64. Guynet, C. & De La Cruz, F. 2011. Plasmid segregation without partition. *Mob Genet Elements*, 1, 236-241
65. Sun, X., Chen, X. J., Feng, J., Zhao, J. Y. & Li, Y. Z. 2011. Characterization of the partitioning system of Myxococcus plasmid pMF1. *PLoS One*, 6, e28122.
66. Summers, D. K. 1991. The kinetics of plasmid loss. Trends Biotechnol, 9, 273-8.

67. Glick, B. R. 1995. Metabolic load and heterologous gene expression. *Biotechnol Adv*, 13, 247-61.
68. Friehs, K. 2004. Plasmid copy number and plasmid stability. *Adv Biochem Eng Biotechnol*, 86, 47-82.
69. Tsang, J. 2017. Bacterial plasmid addiction systems and their implications for antibiotic drug development. *Postdoc J*, 5, 3-9.
70. Wen, Y., Behiels, E. & Devreese, B. 2014. Toxin-Antitoxin systems: their role in persistence, biofilm formation, and pathogenicity. *Pathog Dis*, 70, 240-9.
71. Lesic, B., Zouine, M., Ducos-Galand, M., Huon, C., Rosso, M. L., Prévost, M. C., Mazel, D. & Carniel, E. 2012. A natural system of chromosome transfer in Yersinia pseudotuberculosis. *PLoS Genet*, 8, e1002529.
72. Biot, T. & Cornelis, G. R. 1988. The replication, partition and yop regulation of the pYV plasmids are highly conserved in Yersinia enterocolitica and Y. pseudotuberculosis. *J Gen Microbiol*, 134, 1525-34.
73. Dworkin, M. & Falkow, S. 2006. The prokaryotes: a handbook on the biology of bacteria, New York; [London], Springer.
74. Youngren, B., Radnedge, L., Hu, P., Garcia, E. & Austin, S. 2000. A plasmid partition system of the P1-P7par family from the pMT1 virulence plasmid of Yersinia pestis. *J Bacteriol*, 182, 3924-8.
75. Drancourt, M. 2012. Plague in the genomic area. Clin Microbiol Infect, 18, 224-30.
76. Georgiades, K. & Raoult, D. 2011. Genomes of the most dangerous epidemic bacteria have a virulence repertoire characterized by fewer genes but more toxin-antitoxin modules. *PLoS One*, 6, e17962.
77. Bibi-Triki, S., Li De La Sierra-Gallay, I., Lazar, N., Leroy, A., Van Tilbeurgh, H., Sebbane, F. & Pradel, E. 2014. Functional and structural analysis of HicA3-HicB3, a novel toxin-antitoxin system of Yersinia pestis. *J Bacteriol*, 196, 3712-23.
78. Pilla, G. & Tang, C. M. 2018. Going around in circles: virulence plasmids in enteric pathogens. *Nat Rev Microbiol*, 16, 484-495.
79. Masai, H. & Arai, K. 1987. RepA and DnaA proteins are required for initiation of R1 plasmid replication in vitro and interact with the oriR sequence. *Proc Natl Acad Sci U S A*, 84, 4781-5.
80. Schumacher, M. A., Tonthat, N. K., Kwong, S. M., Chinnam, N. B., Liu, M. A., Skurray, R. A. & Firth, N. 2014. Mechanism of staphylococcal multiresistance plasmid replication origin assembly by the RepA protein. *Proc Natl Acad Sci U S A*, 111, 9121-6.
81. Knittel, V., Vollmer, I., Volk, M. & Dersch, P. 2018. Discovering RNA-Based Regulatory Systems for. *Front Cell Infect Microbiol*, 8, 378.
82. Wang, H., Avican, K., Fahlgren, A., Erttmann, S. F., Nuss, A. M., Dersch, P., Fallman, M., Edgren, T. & Wolf-Watz, H. 2016. Increased plasmid copy number is essential for Yersinia T3SS function and virulence. *Science*, 353, 492-5.
83. Blomberg, P., Nordström, K., Gerhart, E., Wagner, H. 1992. Replication control of plasmid R1: RepA synthesis is regulated by copA RNA through inhibition of leader peptide translation. *The EMBO Journal 11* (7), pp.2675-2683

84. Bower, D. M. & Prather, K. L. 2012. Development of new plasmid DNA vaccine vectors with R1-based replicons. *Microb Cell Fact*, 11, 107.
85. Williams, P. 2007. Quorum sensing, communication and cross-kingdom signalling in the bacterial world. *Microbiology*, 153, 3923-38.
86. Atkinson, S., Goldstone, R. J., Joshua, G. W. P., Chang, C.-Y., Patrick, H. L., Cámara, M., Wren, B. W. & Williams, P. 2011. Biofilm Development on Caenorhabditis elegans by Yersinia Is Facilitated by Quorum Sensing-Dependent Repression of Type III Secretion. *PLoS Pathogens*, 7.
87. Chong, G., Kimyon, O. & Manefield, M. 2013. Quorum Sensing Signal Synthesis May Represent a Selective Advantage Independent of Its Role in Regulation of Bioluminescence in Vibrio fischeri. *PLoS One*, 8, e67443.
88. Ng, Y., Grasso, M., Wright, V., Garcia, V., Williams, P., & Atkinson, S. 2018. The Quorum Sensing System of Yersinia enterocolitica 8081 Regulates Swimming Motility, Host Cell Attachment, and Virulence Plasmid Maintenance. *Genes,* 9.
89. Williams, P., Winzer, K., Chan, W. C. & Cámara, M. 2007. Look who's talking: communication and quorum sensing in the bacterial world. *Philos Trans R Soc Lond B Biol Sci*, 362, 1119-34.
90. Fuqua, C., Parsek, M. R. & Greenberg, E. P. 2001. Regulation of gene expression by cell-to-cell communication: acyl-homoserine lactone quorum sensing. *Annu Rev Genet*, 35, 439-68.
91. Prescott, R. D. & Decho, A. W. 2020. Flexibility and Adaptability of Quorum Sensing in Nature. *Trends Microbiol*, 28, 436-444.
92. Wang, Z., Wu, X., Peng, J., Hu, Y., Fang, B. & Huang, S. 2014. Artificially constructed quorum-sensing circuits are used for subtle control of bacterial population density. *PLoS One*, 9, e104578.
93. Stevens, A. M. & Greenberg, E. P. 1997. Quorum sensing in Vibrio fischeri: essential elements for activation of the luminescence genes. *J Bacteriol*, 179, 557-62.
94. Rutherford, S. T. & Bassler, B. L. 2012. Bacterial quorum sensing: its role in virulence and possibilities for its control. *Cold Spring Harb Perspect Med*, 2.
95. Papenfort, K. & Bassler, B. L. 2016. Quorum sensing signal-response systems in Gram-negative bacteria. *Nat Rev Microbiol*, 14, 576-88.
96. Kirwan, J. P., Gould, T. A., Schweizer, H. P., Bearden, S. W., Murphy, R. C. & Churchill, M. E. 2006. Quorum-sensing signal synthesis by the Yersinia pestis acyl-homoserine lactone synthase YspI. *J Bacteriol*, 188, 784-8.
97. Atkinson, S., Throup, J.P., Stewart, G.S.A.B. and Williams, P. 1999. A hierarchical quorum-sensing system in Yersinia pseudotuberculosis is involved in the regulation of motility and clumping. *Molecular Microbiology*. 33(6), pp.1267–1277.
98. Atkinson, S., Chang, C.-Y., Patrick, H.L., Buckley, C.M.F., Wang, Y., Sockett, R.E., Cámara, M. and Williams, P. 2008. Functional interplay between the Yersinia pseudotuberculosis YpsRI and YtbRI quorum sensing systems modulates swimming motility by controlling expression of flhDC and fliA. *Molecular Microbiology*. 69(1), pp.137–151.

99. Atkinson, S., Chang, C. Y., Sockett, R. E., Cámara, M. & Williams, P. 2006. Quorum sensing in Yersinia enterocolitica controls swimming and swarming motility. *J Bacteriol*, 188, 1451-61.
100. Slater, A. 2017. Unraveling the regulatory relationship between quorum sensing and the type III secretion system in Yersinia pseudotuberculosis. PhD Thesis, University of Nottingham
101. Skurnik M, Toivanen P. LcrF is the temperature-regulated activator of the yadA gene of Yersinia enterocolitica and Yersinia pseudotuberculosis. J Bacteriol. 1992;174(6):2047-51.
102. Lambert de Rouvroit C, Sluiters C, Cornelis GR. Role of the transcriptional activator, VirF, and temperature in the expression of the pYV plasmid genes of Yersinia enterocolitica. Mol Microbiol. 1992;6(3):395-409.
103. Cornelis GR, Sluiters C, Delor I, Geib D, Kaniga K, Lambert de Rouvroit C, et al. ymoA, a Yersinia enterocolitica chromosomal gene modulating the expression of virulence functions. Mol Microbiol. 1991;5(5):1023-34.
104. Irwin PL, Nguyen LH, Paoli GC, Chen CY. Evidence for a bimodal distribution of Escherichia coli doubling times below a threshold initial cell concentration. BMC Microbiol. 2010;10:207.
105. Dai, Q., Xu, L., Xiao, L., Zhu, K., Song, Y., Li, C., Zhu, L., Shen, X. & Wang, Y. 2018. RovM and CsrA Negatively Regulate Urease Expression in Yersinia pseudotuberculosis. *Frontiers in Microbiology*.
106. Hanahan, D. 1983. Studies on transformation of Escherichia coli with plasmids. *Journal of Molecular Biology*, 1664, 557 - 580.
107. Simon, R., Priefer, U. and Puhler, A. 1983. A broad host range mobilization system for in vivo genetic-engineering transposon mutagenesis in Gram-negative bacteria. *Bio-Technology*. 1(9), pp.784–791
108. Stewart, G.S.A.B., Lubinsky-Mink, S., Jackson, C.G., Cassel, A. and Kuhn, J. 1986. pHG165: A pBR322 copy number derivative of pUC8 for cloning and expression. *Plasmid*. 15(3), pp.172–181.
109. Rosqvist, R., Skurnik, M. and Wolf-Watz, H. 1988. Increased virulence of Yersinia pseudotuberculosis by two independent mutations. *Nature*. 334(6182), pp.522– 524.
110. Wiechmann, A. 2015. Quorum Sensing and the Regulation of Multicellular Behaviour in Yersinia pseudotuberculosis. PhD Thesis, University of Nottingham.
111. Schagat, T., Paguio, A. & Kopish, K. 2007. Normalizing Genetic Reporter Assays Approaches and Considerations for Increasing Consistency and Statistical Significance. Cell Notes: Promega Corporation.
112. Protocol - How to Ligate Plasmid DNA [Internet]. Addgene.org. [cited 8 August 2020]. Available from: https://www.addgene.org/protocols/dna-ligation/
113. Chang A., Chau V., Landas J., Pang Y. Preparation of calcium competent Escherichia coli and heat-shock transformation. JEMI Methods [Internet]. 2017 [cited 20 September 2020];1:22-25. Available from: https://jemi.microbiology.ubc.ca/sites/default/files/Chang%20et%20al%20JEMI-methods%20Vol%201%20pg%2022-25.pdf

114. Padmanabhan, S., Banerjee, S. & Mandi, N. 2011. Screening of Bacterial Recombinants: Strategies and Preventing False Positives. Molecular Cloning – Selected Applications in Medicine and Biology.
115. Standard PCR Protocol [Internet]. sigmaaldrich.com. [cited 8 August 2020]. Available from: https://www.sigmaaldrich.com/technical-documents/protocols/biology/standard-pcr.html?gclid=CjwKCAjw19z6BRAYEiwAmo64LQ5-9FbsNR8A976XSt5i-dfVzttHbRtZSWNofnru48Vteyb_lplRdhoCEccQAvD_BwE
116. Milton, D. L., O'Toole, R., Horstedt, P. & Wolf-Watz, H. 1996. Flagellin A is essential for the virulence of Vibrio anguillarum. *J Bacteriol*, 178, 1310-9.
117. Casali N, Preston A. E. coli plasmid vectors. 1st ed. Totowa, N.J.: Humana Press; 2003.
118. Blue-White Screening & Protocols for Colony Selection [Internet]. Merck. [cited 20 September 2020]. Available from: https://www.sigmaaldrich.com/technical-documents/articles/biology/blue-white-screening.html
119. Burlage, R. S., Sayler, G. S. & Larimer, F. 1990. Monitoring of naphthalene catabolism by bioluminescence with nah-lux transcriptional fusions. *J Bacteriol*, 172, 4749-57.
120. Beard, S. J., Salisbury, V., Lewis, R. J., Sharpe, J. A. & Macgowan, A. P. 2002. Expression of lux genes in a clinical isolate of Streptococcus pneumoniae: using bioluminescence to monitor gemifloxacin activity. *Antimicrob Agents Chemother*, 46, 538-42.
121. Truchado, P., Giménez-Bastida, J. A., Larrosa, M., Castro-Ibáñez, I., Espín, J. C., Tomás-Barberán, F. A., García-Conesa, M. T. & Allende, A. 2012. Inhibition of quorum sensing (QS) in Yersinia enterocolitica by an orange extract rich in glycosylated flavanones. *J Agric Food Chem*, 60, 8885-94.
122. Vandeputte, O. M., Kiendrebeogo, M., Rasamiravaka, T., Stévigny, C., Duez, P., Rajaonson, S., Diallo, B., Mol, A., Baucher, M. & El Jaziri, M. 2011. The flavanone naringenin reduces the production of quorum sensing-controlled virulence factors in Pseudomonas aeruginosa PAO1. *Microbiology (Reading),* 157, 2120-2132.
123. Dong, Y. H., Xu, J. L., Li, X. Z. & Zhang, L. H. 2000. AiiA, an enzyme that inactivates the acylhomoserine lactone quorum-sensing signal and attenuates the virulence of Erwinia carotovora. *Proc Natl Acad Sci U S A,* 97, 3526-31.
124. Gerdes, K. 2000. Toxin-antitoxin modules may regulate synthesis of macromolecules during nutritional stress. *J Bacteriol*, 182, 561-72.
125. Jiang, Y., Pogliano, J., Helinski, D. R. & Konieczny, I. 2002. ParE toxin encoded by the broad-host-range plasmid RK2 is an inhibitor of Escherichia coli gyrase. *Mol Microbiol*, 44, 971-9.
126. Kamruzzaman, M. & Iredell, J. 2019. A ParDE-family toxin antitoxin system in major resistance plasmids of Enterobacteriaceae confers antibiotic and heat tolerance. *Sci Rep*, 9, 9872.